Improved radionuclide therapy of neuroblastoma

Preclinical evaluation of ^{177}Lu-labeled somatostatin analogs

Arman Romiani

Department of Medical Radiation Sciences
Institute of Clinical Sciences
Sahlgrenska Center for Cancer Research
Sahlgrenska Academy at University of Gothenburg

UNIVERSITY OF GOTHENBURG

Gothenburg 2023

Cover illustration by Arman Romiani

Improved radionuclide therapy of neuroblastoma
- Preclinical evaluation of ^{177}Lu-labeled somatostatin analogs

arman.romiani@gu.se

ISBN: 978-91-8069-153-6 (Print)
ISBN: 978-91-8069-154-3 (PDF)

Printed by Stema Specialtryck AB, Borås, Sweden 2023

"Two little mice fell into a bucket of cream. The first mouse quickly gave up and drowned.

The second mouse, wouldn't quit. He struggled so hard that eventually he churned that cream into butter and crawled out. Gentlemen, as of this moment, I am that second mouse."

Frank Abagnale
Catch Me If You Can (2002)

Abstract

Improved radionuclide therapy of neuroblastoma

Preclinical evaluation of ^{177}Lu-labeled somatostatin analogs

Arman Romiani

Department of Medical Radiation Sciences, Institute of Clinical Sciences
Sahlgrenska Center for Cancer Research, Sahlgrenska Academy
at University of Gothenburg, Sweden

Today, about half of the children diagnosed with high-risk neuroblastoma (HR-NB) survive due to considerable treatment improvements during the last decades. However, there is still much to be done for the other half who are not cured with current treatments. In addition, children with HR-NB often have metastatic spread at diagnosis, requiring systemic treatment.

HR-NBs have some specific biological characteristics that can be targeted for treatment systemically. For example, *ALK* encodes for the anaplastic lymphoma kinase receptor found mutated in about 15% of HR-NBs. Another example is somatostatin receptors (SSTRs), expressed between 60-90% in all NBs. These SSTRs can be targeted with ^{177}Lu-labeled somatostatin analogs (e.g., ^{177}Lu-octreotate and ^{177}Lu-octreotide). In addition, patients with SSTR-overexpressing gastroenteropancreatic neuroendocrine tumors (NETs) are treated with ^{177}Lu-octreotate. However, the usefulness of ^{177}Lu-labeled somatostatin analogs in HR-NB patients has yet to be thoroughly investigated.

The aim of this work was to evaluate the therapeutic usefulness of ^{177}Lu-labeled somatostatin analogs from studies on HR-NB cell lines and HR-NB xenograft mouse models.

Experiments performed on two different HR-NB cell lines demonstrated high specific binding and internalization of ^{177}Lu-octreotate compared to other cell lines of various tumor types. This led to further studies in mouse models. NB-bearing BALB/c nude mice were administered different amounts of ^{177}Lu-octreotate or ^{177}Lu-octreotide, and the biodistribution was studied in various tissues. Biodistribution data analysis demonstrated a relatively high tumor uptake in all three investigated HR-NB mouse models compared with similar studies in other NET mouse models, both for ^{177}Lu-octreotate and ^{177}Lu-octreotide. Dosimetric estimations showed high absorbed dose to tumor tissue.

Subsequent studies included various treatment regimens. In these studies, curative amounts of ^{177}Lu-octreotate or ^{177}Lu-octreotide were administered as single injections, fractionated, or combined with the ALK-inhibitor lorlatinib. Therapeutic effects were determined from tumor volume measurements. In addition, the transcriptional response of specific genes involved in apoptosis was studied using qPCR. Despite high uptake and absorbed dose to tumor, treatment with single injections of ^{177}Lu-octreotate or ^{177}Lu-octreotide led to modest therapeutic effects, where ^{177}Lu-octreotide caused a more substantial anti-tumor effect. In addition, fractionation with ^{177}Lu-octreotate resulted in prolonged survival. However, a synergistic effect was observed when combining lorlatinib and ^{177}Lu-octreotide for the tumor with *ALK* mutation. The combination treatment also led to an elevated apoptotic transcriptional response.

In summary, this thesis demonstrates that ^{177}Lu-labeled somatostatin analogs can be beneficial in the treatment of patients with disseminated HR-NBs overexpressing SSTRs. However, since many HR-NBs may have specific mutations or amplifications, a combination with other drugs (e.g., lorlatinib) might be needed to overcome potential radioresistance and to enhance the anti-tumor effects.

Keywords

Peptide receptor radionuclide therapy, somatostatin receptors, neuroblastoma, internalization, biodistribution, dosimetry, apoptosis, gene expression, lorlatinib

Populärvetenskaplig sammanfattning

Idag överlever ungefär hälften av de barn som diagnostiserats med högrisk neuroblastom (HR-NB). Betydande förbättringar gällande deras behandling har skett under de senaste årtiondena. Dock finns det fortfarande mycket kvar att göra för den andra hälften av barnen som inte botas med de nuvarande behandlingarna. Vid diagnos har oftast sjukdomen spridit sig, vilket kräver en systemisk behandling, som ger möjligheten att nå tumörceller oberoende av var de befinner sig i kroppen. Eftersom HR-NB celler har en stor mängd av somatostatin-receptorer (SSTR) på sin yta, så kan dessa celler angripas med hjälp av tumörsökande substanser, som binder till SSTR. Om man kopplar på ett radioaktivt ämne, exempelvis ^{177}Lu, på den tumörsökande substansen, så har man ett radioaktivt läkemedel. Det radioaktiva läkemedlet kan injiceras i blodet och kommer kunna söka upp spridda tumörceller i kroppen, och bestråla dem på nära avstånd. I detta arbete har två olika radioaktiva läkemedel använts, ^{177}Lu-oktreotat och ^{177}Lu-oktreotid, och båda binder bra till SSTR. Idag använts ^{177}Lu-oktreotat för behandling av patienter med så kallade neuroendokrina tumörer i mag-tarm-kanalen, i de fall då tumörerna uttrycker tillräckligt med SSTR.

Kan dessa radioaktiva läkemedel användas för behandling av barn med HR-NB?

Det är denna frågeställning som lagt grunden för avhandlingen. För att kunna svara på den frågan har ett flertal studier genomförts pre-kliniskt, vilket innefattar studier utförda på mänskliga HR-NB celler och på möss bärandes på mänskligt HR-NB. Det övergripande målet har varit att utvärdera möjligheten av denna nya typ av behandling.

Experimenten utfördes på två olika HR-NB cellinjer för att undersöka om det finns ett specifikt upptag av ^{177}Lu-oktreotat. Dessa experiment påvisade ett specifikt upptag av ^{177}Lu-oktreotat i de studerade HR-NB cellinjerna. Fortsatta experiment genomfördes på tre olika musmodeller. I dessa musmodeller injicerades olika mängder av ^{177}Lu-oktreotat eller ^{177}Lu-oktreotid, för att sedan studera hur det radioaktiva läkemedlet spridit sig till olika vävnader. Här kunde relativt höga upptag av de

radioaktiva ämnena detekteras i tumörvävnaden i förhållande till de andra vävnaderna i musmodellerna. Efterföljande studier inriktade sig mer åt terapieffekter med olika behandlingssätt. I dessa studier injicerades större mängder ^{177}Lu-oktreotat eller ^{177}Lu-oktreotid som enstaka injektioner, eller som ett flertal injektioner (fraktioner) eller i kombination med ett annat läkemedel (lorlatinib). Trots det relativt höga upptaget i tumörvävnaden, ledde behandlingarna med de enstaka injektionerna till blygsamma terapieffekter. Däremot fick mössen som fått ett flertal injektioner (fraktioner) en förlängd överlevnad. Det behandlingssätt som gav störst terapieffekt var den när ^{177}Lu-oktreotid kombinerades med läkemedlet lorlatinib.

Sammanfattningsvis visar denna avhandling att radioaktiva läkemedel som binder till SSTR kan vara fördelaktiga vid behandling av patienter med spridd HR-NB som överuttrycker SSTR. Eftersom HR-NB oftast har vissa mutationer eller amplifikationer kan det dock behövas en kombination med andra läkemedel (t.ex. lorlatinib) för att övervinna dess behandlingsresistenta egenskaper för att öka terapieffekterna.

List of papers

This thesis is based on the following four studies, referred to in the text by their Roman numerals.

I. S. Saadati, J. Spetz, V. Sandblom, E. Schüler, A. Romiani, E. Shubbar, D.E. Lind, R.H. Palmer, B. Hallberg, T. Parris, K. Helou, E. Forssell-Aronsson.
Binding and internalization of ^{177}Lu-octreotate in cell lines of neuroblastoma, breast cancer, and non-small cell lung cancer. *Submitted*

II. A. Romiani, J. Spetz, E. Shubbar, D.E. Lind, B. Hallberg, R.H. Palmer, E. Forssell-Aronsson.
Neuroblastoma xenograft models demonstrate the therapeutic potential of ^{177}Lu-octreotate. Accepted for publication in BMC Cancer 2021; 21:950

III. A. Romiani, K. Simonsson, D. Pettersson, A. Al-Awar, N. Rassol, H. Bakr, D.E. Lind, G. Umapathy, K. Helou, R.H. Palmer, B. Hallberg, E. Forssell-Aronsson.
Comparison between ^{177}Lu-octreotate and ^{177}Lu-octreotide in neuroblastoma-bearing mice: biodistribution, therapeutic effects and influence on apoptosis-related genes. *Manuscript*

IV. A. Romiani, D. Pettersson, K. Simonsson, H. Bakr, D.E. Lind, R.H. Palmer, B. Hallberg, K. Helou, E. Forssell-Aronsson.
Synergistic antitumor effects of ^{177}Lu-octreotide combined with an ALK inhibitor in a high-risk neuroblastoma xenograft model. *Manuscript*

The author's contribution

Paper I The author contributed to the data analysis and interpretation and was responsible for the processing of the immunohistochemical-images. The author was one of the co-authors of the manuscript.

Paper II The author was significantly involved in designing and conceptualizing the study. The author was involved in the animal experiments, the following data analysis and interpretation. The author wrote the original draft and was the main author of the paper.

Paper III The author was considerably involved in planning and conceptualizing the study. Specifically, the author was involved in animal experiments and responsible for the following RNA extractions, and the author was also involved in the data analysis and interpretation. Finally, the author wrote the original draft and was the first author of the manuscript.

Paper IV The author was responsible for the study design and implementation. In addition, the author was involved in the data interpretation. The author wrote the original draft and was the first author of the manuscript.

Selection of related presentations

1. Romiani A, Spetz J, Schüler E, Wan H, Palmer R.H, Hallberg B, Forssell-Aronsson E: **Biodistribution of Lu-177-octreotate in nude mice with human neuroblastoma tumors**. *The 35th Annual meeting of Nordic Society of Paediatric Hematology and Oncology*, Stockholm, Sweden, May, 2017.

2. Romiani A, Spetz J, Lind D.E, Wan H, Palmer R.H, Hallberg B, Forssell-Aronsson E: **Therapeutic potential of ^{177}Lu-octreotate for neuroblastoma – preclinical studies**. *The 63rd Annual Meeting of the Radiation Research Society*, Cancun, Mexico, October, 2017.

3. Romiani A, Spetz J, Lind D.E, Shubbar E, Palmer R.H, Hallberg B, Forssell-Aronsson E: **Better therapeutic results after fractionated administration of ^{177}Lu-octreotate in mice bearing human neuroblastoma.** *The 31st Annual Congress of European Association of Nuclear Medicine*, Düsseldorf, Germany, October, 2018.

4. Romiani A, Spetz J, Shubbar E, Palmer R.H, Hallberg B, Forssell-Aronsson E: **Fractionated administration of ^{177}Lu-octreotate in CLB-BAR xenografted nude mice resulted in a better anti-tumor effect**. *Cancerfondens riksplaneringsgrupp för onkologisk radionuklidterapi, Höstmöte*, Gothenburg, Sweden, December, 2019.

5. Romiani A, Pettersson D, Al-Awar A, Rassol N, Bakr H, Lind D. E, Umapathy G, Palmer R.H, Hallberg B, Forssell-Aronsson E: **A comparative study of ^{177}Lu-octreotate and ^{177}Lu-octreotide in neuroblastoma-bearing mice.** *Swedish academic initiative for radiation sciences and nuclear technology*, Stockholm, Sweden, August, 2022.

6. Romiani A, Pettersson D, Al-Awar A, Rassol N, Bakr H, Lind D. E, Umapathy G, Palmer R.H, Hallberg B, Forssell-Aronsson E: **Dose-response effects of ^{177}Lu-octreotide and ^{177}Lu-octreotate in neuroblastoma-bearing mice.** *The 47th Annual Meeting of the European Radiation Research Society*. Catania, Italy, September, 2022.

Table of Contents

Abbreviations

A	Activity
Bq	Becquerel
ALK	Anaplastic lymphoma kinase
ASCT	Autologous stem cell transplantation
CDKs	Cyclin-dependent kinases
DDRs	DNA damage responses
DMSO	Dimetylsulfoxid
DNA	Deoxyribonucleic acid
DOTA	Dodecanetetraacetic acid
DSBs	Double-strand breaks
eV	Electron volt
FADD	Fas-associated death domain
Ga	Gallium
GO	Gene Ontology
Gy	Gray
Hf	Hafnium
HR-NB	High-risk neuroblastoma
I	Iodine
IA	Injected activity
IDRFs	Image-defined risk factors
IHC	Immunohistochemical
In	Indium
INRG	International Neuroblastoma Risk Group
ITLC	Instant thin layer chromatography
LET	Linear energy transfer
Lu	Lutetium
mIBG	Metaiodobenzylguanidine
MIRD	Medical Internal Radiation Dose Committee
MOMP	Mitochondrial outer membrane permeabilization
mRNA	Messenger RNA
NB	Neuroblastoma
NETs	Neuroendocrine tumors
NSCLC	Non-small-cell lung cancer
OAR	Organs at risk
PET	Positron emission tomography

PFS	Progression-free survival
PRRT	Peptide receptor radionuclide therapy
qPCR	Quantitative polymerase chain reaction
RNA	Ribonucleic acid
RTK	Receptor tyrosine kinase
RTV	Relative tumor volume
SEM	Standard error of the mean
SI-NET	Small intestine neuroendocrine tumor
SPECT	Single-photon emission computerized tomography
SSBs	Single-strand breaks
SSTAs	Somatostatin analogs
SSTRs	Somatostatin receptors
T/N	Tumor-to-normal-tissue activity concentration ratio
TNF	Tumor necrosis factor
Tyr	Tyrosine

Background

Peptide receptor radionuclide therapy (PRRT) is a systemic treatment using radiopharmaceuticals that targets peptide receptors to deliver localized treatment. For many neuroendocrine tumors (NETs), PRRT is a treatment option due to an elevated expression of somatostatin receptors (SSTRs) in many NET types. Through tumor-seeking agents, somatostatin analogs (SSTAs), bound radionuclides can be delivered to tumor cells that over-express SSTRs. Furthermore, depending on the choice of radionuclide, the tumor can be visualized, eradicated, or both. Due to these beneficial properties, Radiolabeled SSTAs have been implemented for more than 30 years to treat patients with metastatic or inoperable SSTR-positive NETs [1]. With time, improvements have been made in PRRT through the development of radiopharmaceuticals and the characterization of biological tumor properties. As the advantages of PRRT have become more evident, questions have been raised about its usefulness for other malignancies, highlighting the need for a thorough analysis of the treatment as a whole and to identify possible optimization aspects.

Neuroblastoma

Neuroblastoma (NB) represents 7-9% of all tumors detected in children [2, 3] and is one of the most frequently diagnosed tumor types in infants. NB, classified as a NET, is derived from primitive nerve cells in the sympathetic nervous system. Approximately two-thirds of the primary NBs are localized to the adrenal medulla [3]. In patients with disseminated disease, metastases are most commonly located in the regional lymph nodes, bone marrow, skeleton, liver, and skin [4]. NB is a heterogeneous malignancy with various biological characteristics and, thus, diverse clinical outcomes. Therefore, NB patients are divided into risk-assessment groups based on the localization of metastases and tumor-specific features. Patients with high-risk NBs (HR-NB) have an overall survival of less than 50%, while survival rates are around 90-100% for low-risk NB patients [2, 5, 6].

The *MYCN* oncogene is amplified in approximately 20% of all NBs and is highly associated with aggressive NBs [4, 7, 8]. Another oncogene is the

anaplastic lymphoma kinase (*ALK*) gene, in which mutations are found in up to 15% of newly diagnosed HR-NB [7]. Both *MYCN* and *ALK* are thus useful biomarkers for NB tumor aggressiveness. Furthermore, the child´s age, tumor histology, 11q deletion, and DNA ploidy are used for disease classification (**Table 1**).

An International Neuroblastoma Risk Group (INRG) Staging System was developed to form an unanimous approach to pre-treatment risk stratification. Monclair et al. introduced and recommended that the disease should be categorized based on diagnostic images [9]. The emphasis was on so-called image-defined risk factors (IDRFs), illustrating the tumor's relationship to vital structures, i.e., tumors encasing parts of the artery, spinal cord, or trachea. In the absence of these IDRFs in combination with locoregional disease, a classification was made for the first INRG steps, L1 and L2, respectively.

Table 1. International Neuroblastoma Risk Group (INRG) Consensus Pretreatment

INRG Stage	INRGSS Description	Age (months)	Histologic Category	Grade of Tumor differentiation	*MYCN*	11q- del.	Ploidy		Pretreatment Risk Group
L1/L2			GN maturing; GNB intermixed					A	Very low
L1	Localized tumor not involving vital structures as defined by the list of image-defined risk factors* and confined to one body compartment		Any, except GN maturing or GNB intermixed		NA			B	Very low
					Amp			K	High
L2	Locoregional tumor with presence of one or more image-defined risk factors	<18	Any, except GN maturing or GNB intermixed		NA	No		D	Low
						Yes		G	Intermediate
		≥18	GNB nodular; neuroblastoma	Differentiating	NA	No		E	Low
						Yes		H	Intermediate
				Poorly/underdiff.	NA				
					Amp			N	High
M	Distant metastatic disease (except stage MS)	<18			NA		Hyperpl.	F	Low
		<12			NA		Diploid	I	Intermediate
		12-18			NA		Diploid	J	Intermediate
		<18			Amp			O	High
		≥18						P	High
MS	Metastatic disease in children younger than 18 months with metastases confined to skin, liver, and/or bone marrow	<18			NA	No		C	Very low
						Yes		Q	High
					Amp			R	High

Very low risk (5-year event-free survival >85%); low risk (75-85%); intermediate risk (50-75%); high risk (<50%). GN, ganglioneuroma; GNB, ganglioneuroblastoma; Amp, amplified; NA, not amplified. Table adapted from Monclair et al., Cohn et al., and Fransson [9-11]. *Risk factors presented in Monclair et al. [9].

Then, stage M was stated for disseminated disease, followed by stage MS for metastasis to specific organs, followed by an age criterion of fewer than 18 months (**Table 1**). Further, recommendations were made for a more standardized strategy for molecular diagnostic testing of NB tumor tissue.

Surgery alone results in favorable prognoses for patients with resectable low-risk NB. However, approximately 50% of children with neuroblastoma have metastases when the disease is diagnosed, restricting the surgical option [12]. For patients with HR-NB, multimodal therapy, including surgery, chemotherapy, external radiation therapy, radionuclide therapy, ALK-inhibitors, and autologous peripheral blood stem cell transplantation, is included [8]. Despite various treatment options, survival rates for HR-NB patients remain low, further emphasizing the need for novel treatment options.

n-Myc

Most malignancies possess a dysregulated transcription factor within the Myc family [13]. An overexpression of n-Myc has been observed in astrocytoma, glioblastoma, neuroendocrine prostate cancer, small-cell lung cancer, and neuroblastoma [5, 14-17]. Clinical data have demonstrated a strong correlation between *MYCN* amplification and the development of HR-NB; hence *MYCN* has been assessed as a biomarker to categorize the disease [18, 19]. *MYCN* plays a crucial role in many aspects required for malignancy to occur and to keep HR-NB cells in a stem-like state [5, 20, 21]. More specifically, n-Myc forms a complex with Max (a transcription regulator) and binds to the DNA at a specific sequence to activate the transcription of genes involved in, e.g., survival, proliferation, self-renewal, angiogenesis, and metastasis [5, 22, 23]. n-Myc/Max can also suppress genes that promote cell cycle arrest, differentiation, and immune response [5, 23]. This aligns with the fact that several studies have shown that NB possesses a cell population with stem-cell-like properties [24-28], defined as a subpopulation within the tumor that is highly malignant, treatment-resistant, and with the ability to self-renewal [29, 30]. In addition, n-Myc has also been shown to regulate NB cells towards radioresistance [31]. Despite the knowledge of its prominent role, there are currently no drugs for clinical use that can restrain or regulate the function of n-Myc. As for inhibiting other transcription factors, difficulty arises in aiming at specific targets within the nucleus instead of the cell membrane or in the cytoplasm [32]. One possible explanation is that interactions within the nucleus require cooperation between multiple low-affinity complexes, creating a challenging path for the drug to reach the correct site [32]. Further, the molecular similarities of n-Myc to other Myc proteins is an additional challenge, since c-Myc is necessary for cell

division in normal tissues, the proposed drug needs to be remarkably selective in order to avoid toxicity in normal tissues [32, 33].

ALK

ALK is a member of the insulin receptor tyrosine kinase (RTK) superfamily and is involved in developing the neonatal nervous system [34, 35]. Amplification, oncogenic mutations, or gene translocations of *ALK* have been linked to various tumor types such as non-small-cell lung cancer (NSCLC), anaplastic large-cell lymphoma, and NB [35]. In addition, altered ALK structures can lead to constitutive autophosphorylation and activation associated with poor clinical outcomes, present in approximately 15% of newly diagnosed HR-NBs [7, 36-39]. Most of the verified *ALK* mutations lead to altered ALK structures in the intracellular part, specifically within the kinase domain [40, 41]. In neuroblastoma, *ALK* is mainly activated through point mutations, where three hotspots represent approximately 85% of all *ALK* mutations [39]. These gain-of-function mutations increase the ALK downstream signaling pathways, affecting, e.g., proliferation, angiogenesis, cell cycle arrest, and apoptosis [35, 41, 42]. *ALK* mutations correlate with *MYCN* amplification, and preclinical studies have shown their cooperation in the development of NB [43-45]. Additionally, ALK can induce transcription of *MYCN* in NB, indicating why NB patients with *ALK* mutations and *MYCN* amplification have enhanced lethality [43]. Unlike the Myc family, ALK is not as well distributed and expressed in normal tissue, making it a suitable target for treatment [34, 46, 47].

Significant efforts have been made in the past decades to develop ALK-inhibitors (ALKis). ALKis bind to the ATP binding site in the tyrosine kinase domain, thus preventing autophosphorylation and activation of ALK. Categorized as the first-generation of ALKis, Crizotinib (PF-02341066) was FDA-approved in 2011 for patients with metastatic ALK-positive NSCLC [48]. Most patients responded initially to Crizotinib, and it was demonstrated that Crizotinib significantly enhanced progression-free survival (PFS) from 3.0 to 7.7 months compared with other chemotherapies [49]. Unfortunately, patients later began to develop resistance to Crizotinib [50]. More specifically, it was demonstrated that specific *ALK* mutations led to the structural alteration within the ATP-binding site that prevented binding to Crizotinib [50]. Guided by this finding, more efficient ALKis were developed, such as Ceritinib (LDK-378), Alectinib (CH5424802), and Brigatinib (AP26113), all categorized as

second-generation ALKis [51-53]. Next-generation ALKis were introduced and they would target specific mutations identified from biopsies taken from ALKi-resistant patients [54, 55]. Lorlatinib (PF-06463922), categorized as the third-generation of ALKi, is highly potent and efficient against identified ALKi-resistant mutants in NSCLC and NB [56-59]. However, despite the encouraging results, both preclinically and clinically, drug resistance still remains a recurring problem. Studies have indicated that resistance may also arise from bypassing ALK signaling via the activation of other RTKs. Signaling pathways via the epidermal growth factor receptor (EGFR), ErbB4, and RAS have been demonstrated as bypassing tracks in the development of ALKi resistance [60-62]. Therefore, understanding the mechanisms leading to resistance is critical to developing better therapeutic options. This can be done by precise molecular characterization of *ALK* mutations before and during treatment to follow up on new mutations that may occur during treatment. In addition, the information from the molecular characterization can be applied during treatment to determine the most potent ALKi. Another strategy is to combine ALKis with other drugs that enhance the anti-tumor effects, eradicating a more significant proportion of the tumor population and reducing the risk of relapse.

Radiopharmaceuticals

Prior research show that local radiotherapy of HR-NB patients led to promising results [63-66]. However, the heterogeneous characteristics of NBs make it difficult to draw general conclusions. Nevertheless, HR-NB is usually metastasized, thus limiting effectiveness of external beam radiotherapy [12]. Therefore, another approach is molecular radiotherapy, where radiopharmaceuticals are administered systemically and can target multiple sites and irradiate the tumor cells. This is possible since NB cells overexpress a variety of molecular targets that radiopharmaceuticals can pinpoint for localization and treatment.

Targeting NATs

Expression of noradrenaline transporters (NATs) is found in approximately 85-90% in all NBs, enabling the role of a molecular target [67]. Diagnosis and therapy using the noradrenaline analog metaiodobenzylguanidine (mIBG) is an already established radiopharmaceutical option for patients with NB. The radionuclides ^{123}I (ɤ

emitter), or ^{131}I (β^- and γ emitter), are bound to mIBG for diagnosis and treatment, respectively [68]. Internalization of mIBG into NET cells can occur in two different ways: Most predominantly is an active process via NATs on the cell surface. In contrast, the other way is non-specific diffusion [69, 70]. For most NET cells, the intracellular distribution of mIBG looks similar. The mIBG is stored in neurosecretory granules (e.g., pheochromocytoma) [71]. However for NB cells, mIBG is also accumulated in the mitochondria [70, 72]. Scintigraphy using ^{123}I-mIBG is today an established method for tumor localization. For tumor treatment, ^{131}I-mIBG gave the first successful results in the 1980s [73, 74]. ^{131}I-mIBG therapy has response rates of 20-37% in patients with refractory and relapsed NB [75, 76]. To prevent side effects after ^{131}I-mIBG therapy and intense chemotherapy, such as myelosuppression, patients may undergo autologous stem cell transplantation (ASCT) [77]. The need for ASCT depends on the intensity of the treatments. Although studies have demonstrated variable results for ^{131}I-mIBG therapy versus other cytotoxic drugs, ^{131}I-mIBG exists as a treatment option for HR-NB patients [68, 78].

Targeting SSTRs

Another molecular target is SSTRs, included in the G-protein coupled receptor family, which enables the use of radiolabeled SSTAs. Based on various clinical studies where the specific uptake of radiolabeled SSTAs was assessed, SSTRs were expressed in approximately 60-90% of all NBs [79-81]. All SSTR subtypes (SSTR1-5) have been detected in NB patients. However, low SSTRs expression correlates with the most advanced stages of HR-NBs [80, 82, 83]. Receptor subtype SSTR2 is among the subtypes expressed more frequently and where expression also appears to persist in relapsed NB [82, 84]. In addition, most of the clinically available SSTAs have the highest affinity towards SSTR2 due to the frequent overexpression of this subtype also in other NETs [85, 86]. Octreotide and octreotate are two examples of SSTAs commonly used as receptor-binding carrier molecules. In comparison, the latter shows a slightly higher affinity towards SSTR2 and a lower affinity towards SSTR3 [85]. SSTAs are conjugated to a chelator, e.g., DOTA (Dodecane Tetraacetic Acid), to various radionuclides depending on a diagnostic or therapeutic purpose. For example, for diagnostic purposes, ^{68}Ga-DOTA-octreotate, β^+-emitter, has been developed for positron emission tomography (PET) in order to localize the tumor and eventual metastases. ^{68}Ga-DOTA-octreotate may

be used as an adjunct diagnostic radiopharmaceutical for patients with NB where tumor localization is not feasible with radiolabeled mIBG [87-89].

For treatment, ^{177}Lu (β- and ɤ-emitter) is commonly used due to its suitable physical properties [90]. The emitted particles of ^{177}Lu can be implemented for diagnostics and treatment, subsequently, ^{177}Lu decays to the stable ground state of ^{177}Hf (**Figure 1**). The range of the emitted beta particles corresponds to a maximum of 1.9 mm in water, with a mean range of 0.25 mm [91]. Thus, the emitted beta particles are well suited to eradicate metastatic tumors. Furthermore, the photons emitted may also be used to monitor the therapeutic response and for patient dosimetry.

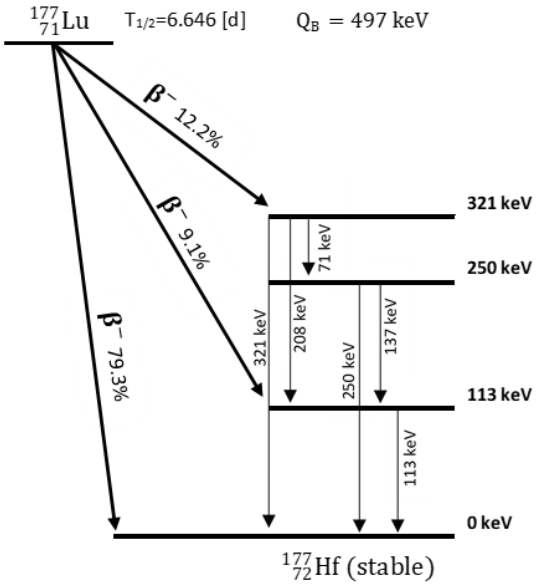

Figure 1. Simplified decay scheme of ^{177}Lu [92].

Table 2. Decay data for ^{177}Lu. Yields > 1% are presented [92].

^{177}Lu		
Radiation	**Yield (%)**	**Energy (keV)**
ɤ	6.40	113
ɤ	11.0	208
X-ray, Hf $L_{\alpha 1}$	1.15	7.90
X-ray, Hf $L_{\beta 1}$	1.09	9.02
X-ray, Hf $K_{\alpha 2}$	1.62	54.6
X-ray, Hf $K_{\alpha 1}$	2.83	55.8
β^-	12.2	177
β^-	9.10	385
β^-	79.3	497

The emitted photons may be detected with single-photon emission computerized tomography (SPECT) (**Table 2**). Based on assessments of SPECT images, the mean absorbed dose can be estimated for the tumor and other organs during treatment. Radiolabeled SSTAs are accumulated in some organs beside the tumor. The bone marrow and the kidneys are the two main dose-limiting organs when planning for PRRT [93, 94]. Derived data from external radiotherapy has the tolerance dose of 2 Gy

and 28 Gy for bone marrow and kidneys, respectively [95, 96]. However, studies indicate that these dose levels can be exceeded without any toxic effects being observed [97, 98]. As the organs at risk (OAR) limit the activity levels administered, and affects the treatment scheme and the total treatment period, it is of utmost importance that correct toxicity assessments are made for OAR.

^{177}Lu-DOTA-octreotate (Lutathera) received EMA and FDA approval in 2017 and 2018, respectively, for SSTR-positive small intestine NETs (SI-NETs) after demonstrating an increased PFS in a comprehensive phase 3 trial [99]. Lutathera is administered with up to four fixed cycles of 7.4 GBq, with 6-8 week intervals. Simultaneously, an intravenous amino acid solution is administered for renal protection on each occasion. Lutathera treatment of patients with SSTR-positive NBs has also been proposed in cases with high uptake of ^{68}Ga-DOTA-octreotate, [87, 89, 100]. However, the few clinical studies that have been completed demonstrated variable results [87, 100, 101]. The hypotheses for the absence of anti-tumor effects are proposed to be due to undertreatment of patients and the lengthy time interval between the administrations (two months) [101]. This is because the phase II study was designed according to the guidelines for Lutathera treatment of patients with SI-NETs. However, unlike SI-NET, NB is rapidly proliferating, allowing repopulation between administrations. However, an ongoing phase II study addresses both of these aspects, aiming to personalize Lutathera treatment of patients with SSTR-positive NB [102]. This is planned to be achieved by optimizing the activity levels administered based on biokinetic data from SPECT/CT images, both before and during treatment, and reducing the time interval between treatments (2-4 weeks), while keeping the dose levels below 2.4 Gy and 23 Gy to whole-body and kidney, respectively.

Mechanisms of SSTRs

The mechanisms that prevail after radiolabeled SSTA has bound to SSTRs are of interest to further improve and optimize treatment. The SSTAs that acts as agonists, e.g., octreotide and octreotate, are specifically of interest as after binding to SSTRs they can be internalized [103-105] (**Figure 2**). SSTR2, SSTR3, and SSTR5 are internalized via endocytosis to a greater extent than SSTR1 and SSTR4 [103]. In addition to a rapid internalization (~10 min), SSTR2 also demonstrates relatively fast recycling (~40 min) to the cell membrane [105]. Unlike SSTR3 and SSTR5, which undergo desensitization and, to some extent, degradation after internalization,

SSTR2 is resensitized upon recycling [106]. Temporarily, the internalized radiolabeled SSTA remains in the cell and is suggested to be transported into lysosomes (which also express SSTR2) to be degraded [107, 108].

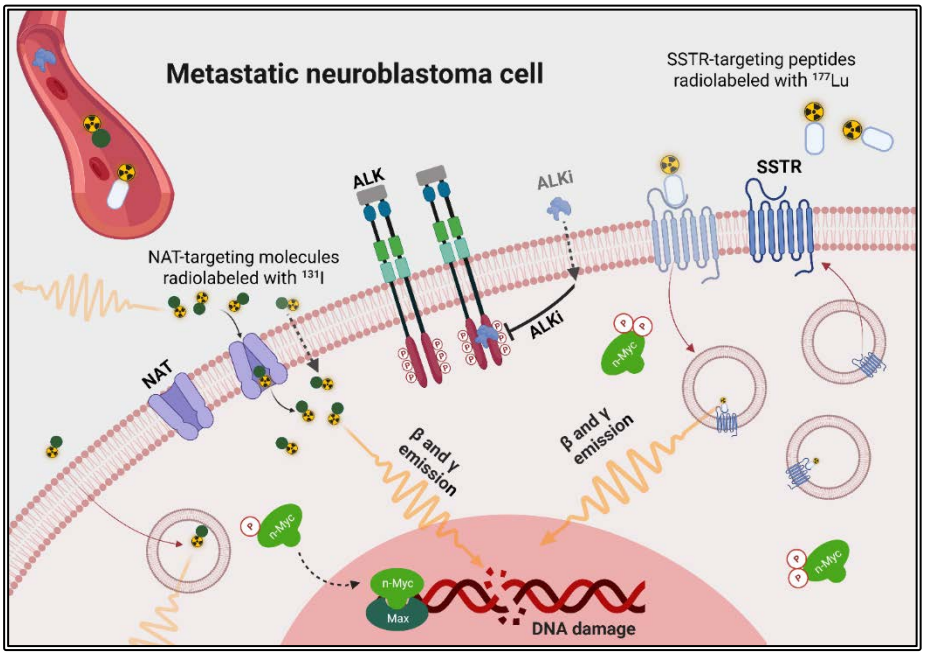

Figure 2. Schematic illustration of different molecular targets in a metastatic neuroblastoma cell. NAT, noradrenaline transporter; SSTR, somatostatin receptor; ALKi, anaplastic lymphoma kinase inhibitor.

SSTAs that act as antagonists, e.g., JR11 and LM3, are not internalized after binding to SSTRs (primarily designed for SSTR2) [109, 110]. Numerous preclinical studies have demonstrated beneficial properties of antagonists both for imaging and treatment, and in recent years, clinical studies have also shown similar benefits [110-115]. The combination of higher affinity towards SSTR2, a larger population of binding sites, and the propensity to remain at the cell membrane leads to elevated tumor uptake, prolonged retention, increased tumor dose, and improved tumor-to-organ dose ratios compared to the corresponding agonists [113, 114]. The favorable aspects indicate a development for using radiolabeled SSTAs with antagonistic properties for SSTR-positive NETs, but to date, none has been clinically approved.

Cellular responses to irradiation

The properties of ionizing radiation have been implemented for various cancers since the early 1900s, aiming to eradicate cancer cells with ionizing radiation while restricting the damage to healthy tissue. The treatments have evolved through numerous developments that have improved radiation therapy. Consequently, our knowledge of the biological effects has also grown, enabling the identification of various cellular responses due to irradiation. In general terms, upon radiation-induced DNA damage, the following possibilities can occur: DNA repair, senescence, cell death, or the cell continues with a chromosomal anomaly [116, 117]. In addition, abnormal division of aneuploid cells may lead to genetic alterations and, thus, development and advancement of cancer [116, 117]. The DNA can be damaged via either direct or indirect ionizing radiation. In the direct effect, the ionizing radiation interacts directly with DNA and ionizes its polynucleotide chains. In the indirect effect, radiation ionizes surrounding molecules, creating reactive species and subsequently affecting DNA [118, 119]. There are several types of DNA damage, and the two more challenging damages to repair are categorized as single-strand breaks (SSBs) and double-strand breaks (DSBs). Irradiations with high linear energy transfer (LET), such as alpha particles and heavy ions, causes more complex DNA damage, mainly DSBs, and have a higher proportion of direct effects on DNA to induce cell death [120]. In contrast, irradiation with lower LET cause less extensive DNA damage, mainly SSBs, and have a more significant impact of indirect effects to cause cell death. These potentially lethal lesions activate DNA damage responses (DDRs) that guide the cell to the subsequent outcomes.

DNA repair

Generally, there are three repair mechanisms to correct SSBs, DNA mismatch repair (MMR), base excision repair (BER), and nucleotide excision repair (NER) [121, 122]. MMR proteins recognize and correct mismatched base pairs due to substitution or deletion generated during DNA replication [121]. Damage to one or a few base pairs is corrected by BER, in contrast to NER, which manages more extensive damage, a longer sequence than just the damaged base pairs is replaced [123, 124].

DSBs are more difficult to repair correctly since no template is left intact, in contrast to SSBs, and therefore considered potentially more toxic than SSBs [125]. Consequently, inducing DSBs is specifically of interest to

achieve enhanced tumor damage. Homologous recombination (HR) and non-homologous end-joining (NHEJ) are the two main DSB repair pathways [126]. HR uses the sequence information from the sister chromatid during replication to recreate the damaged and missing region, thus limiting its availability to the S and G2 phases of the cell cycle [126, 127]. Contrarily, NHEJ is available during all cell cycle phases and "patches" the broken ends together, leading to vital information loss and often mutations [126, 127]. The complexity of the damage has proven to be decisive for the choice of the DSB repair mechanism. Complex DNA lesions with clusters of DSBs, created by high LET radiation, are frequently repaired via HR, whereas low LET-induced DSBs are not as dependent on HR [128].

Some of the crucial proteins involved during the initial DDRs are the DNA-dependent protein kinase, the catalytic subunit (DNA-PKcs), the ataxia-telangiectasia mutated (ATM), the ataxia telangiectasia mutated and Rad3 related (ATR), and the poly(ADP-ribose) polymerase (PARP) family [129-131]. SSBs lead to activated ATR and PARP, while DSBs mainly initiate ATM and DNA-PKcs [129, 132]. Inhibiting DDR-proteins aims to enhance the effects of radiation and overcome radioresistance [133, 134].

Cell cycle arrest

The eukaryotic cell cycle consists of four primary phases: growth and preparation for synthesis (G1), DNA replication (S), growth and preparation for mitosis (G2), and finally, daughter cells are formed after mitosis (M) [135]. In addition, a different phase, G0, exists and is considered a resting phase before the G1 phase and therefore regarded outside the main four cell cycle phases [135]. The cell cycle phase also defines a cell's relative radiosensitivity, with the G2-M phase being the most radiosensitive, less sensitive in the G1 phase, and least sensitive in the later part of the S phase [136]. There are distinct checkpoints that control the cell cycle through the different phases. The two primary checkpoints are between phases G1/S and G2/M, governed by specific proteins categorized as cyclin-dependent kinases (CDKs) [135]. The tumor suppressor protein p53 is crucial in regulating the G1/M checkpoint post-irradiation. Radiation-induced DDR activates the p53 pathway via ATM, which initiates its target proteins, i.e., CDKs, subsequently inducing G1/S arrest [137, 138]. The G2/M checkpoint can be activated via ATM and ATR, independently of the p53 pathway [138]. Most tumor cells have altered or lost their p53 functions, resulting in a damaged G1/S checkpoint.

Therefore, DNA damage repair depends on the CDKs responsible for the G2/M checkpoint [139]. Otherwise, irradiated tumor cells, without correct p53-functions, will enter mitosis with unrepaired DNA damage, resulting in cell death, specifically mitotic catastrophe [140]. *TP53* mutations are rare in NBs, and only found in approximately 2% of tumors [141]. However, *TP53* mutations tend to be more frequent in patients with relapse and are associated with drug- and radioresistance [142, 143].

Senescence

Senescence can occur when the telomeres are shortened to the point where cells no longer divide, and subsequently cells age [144, 145]. Nevertheless, senescence can also occur in normal and tumor cells as the irreversible arrest of the cell cycle upon comprehensive cellular stress caused by radiation [146-150]. Prior research has demonstrated the role of ATM, ATR, p53, and p21 as crucial mediators in senescent-like cells [151-153]. Even though the main focus has been on other cellular response mechanisms, some studies highlight the role of senescence in radioresistance and oncogenesis [154, 155]. For example, a preclinical study illustrated increased tumor growth when tumor cells were co-cultivated with senescence-like fibroblasts [155]. Senescence is arising as a therapeutic target relevant to many diseases. Pro-senescent and anti-senescent treatments display encouraging results in preclinical models, and clinical trials are in progress [156-158]. However, relatively little is known about the mechanism of the tumor microenvironment concerning senescence, and a broader understanding is needed to prevent induced radioresistance and improve radiotherapy of cancer.

Cell death

Cell death is a natural end-stage for every cell. Hence, one of the hallmarks of cancer is the incorrect functioning of relevant mechanisms involved in cell death [159]. Therefore, if the treatments cause cell death, to a more prominent extent, in tumor cells than in normal cells, there is a possibility of eradicating the tumor. Understanding which death mechanisms are activated due to radiation is essential to optimize radiotherapy. In addition, identifying which specific signaling pathways are activated can further enhance the anti-tumor effects of radiation, both alone and in combination with other drugs.

Radiation-induced cell death can generally transpire through a non-apoptotic or an apoptotic pathway. Apoptosis is a programmed and highly conserved mechanism for cell death in most eukaryote cells [160]. It is crucial for tissue development and homeostasis [161]. The proximity of a well-functioning p53 is significant for the proper functioning of apoptosis mechanisms. Conversely, an absent or altered p53 usually leads to cell death via other mechanisms. Various external triggers, i.e. radiation, can activate apoptosis via two main pathways, the extrinsic pathway (death-receptor-mediated) or the intrinsic pathway (mitochondria-mediated). Prior research has demonstrated that both apoptotic pathways can be activated due to irradiation [116, 162, 163].

The extrinsic pathway is often called the death receptor pathway and requires ligand-dependent activation of receptors from the tumor necrosis factor (TNF) receptor superfamily [160, 161]. After death ligand binding, caspase-8, caspase-10, and the adaptor protein Fas-associated death domain (FADD) are recruited, forming a death-inducing signaling complex. After which, the downstream effectors, caspase-3, caspase-6, and caspase-7 are activated via a mitochondria-dependent or a mitochondria-independent pathway (**Figure 3**) [116]. Subsequently, the effectors will activate specific death substrates in the cytoplasm and nucleus. Ultimately, the cell content will be packed into apoptotic bodies and prepared for phagocytosis, completing the apoptotic cell death [116, 160]. In addition, apoptotic cells express phosphatidylserine on the cell surface, which signals their state to neighbor cells [160]. Post irradiation, an upregulation of the expression of TNF receptors has been demonstrated [164, 165].

The mitochondria act as the central regulator of the intrinsic apoptotic pathway. Various stimuli can trigger the intrinsic pathway, collectively leading to mitochondrial outer membrane permeabilization (MOMP), which restricts mitochondrial function. Proteins within the Bcl-2 family mediate MOMP. Members of the Bcl-2 family share one or more of the four characteristic domains of homology referred to as the Bcl-2 homology (BH) domains [166, 167]. Members of the Bcl-2 family are divided into three categories based on their BH domains and their roles, pro-, anti-apoptotic, and effectors [167, 168]. Pro-apoptotic members, BH3-only proteins, include Bad, Bid, Bik, Bim, Bmf, Noxa, Puma, and Hrk [168]. Anti-apoptotic members include Bcl-2, Bcl2A1, Bcl-B, Bcl-W, Bcl-xL, and Mcl1.

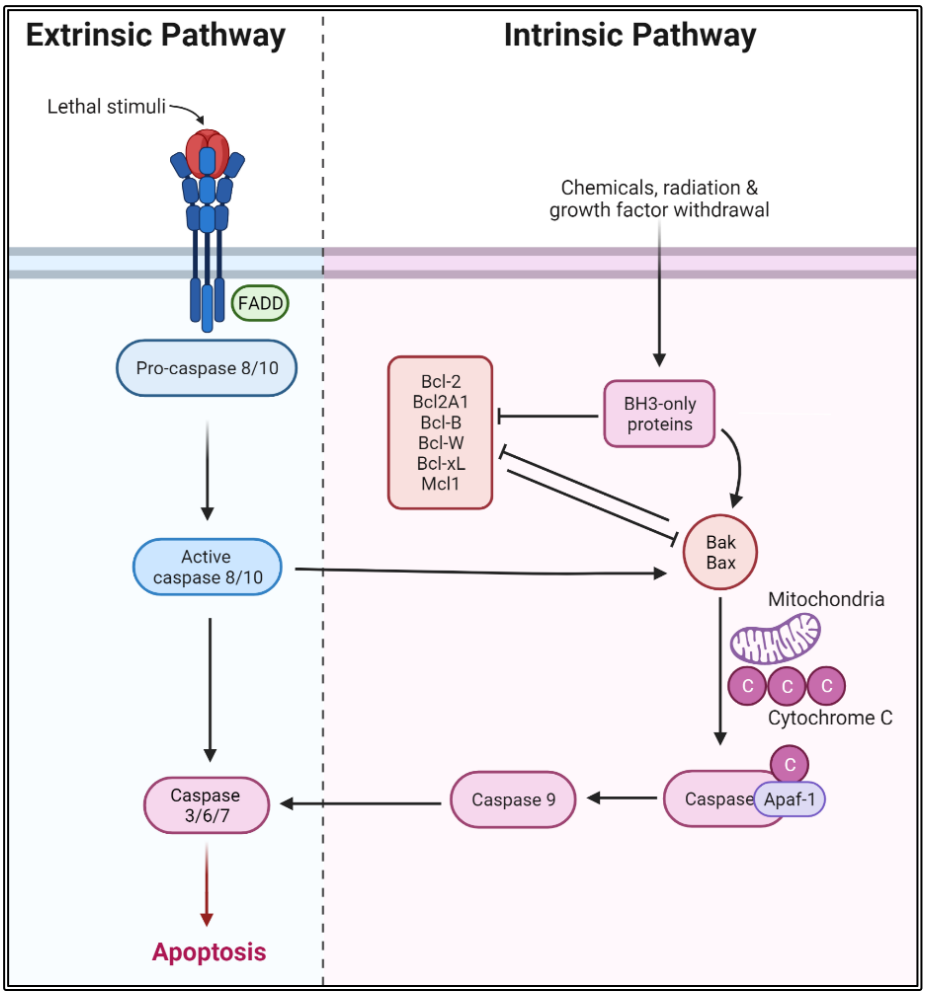

Figure 3. The main steps of apoptosis signaling. Simplified and schematic illustration of the extrinsic and intrinsic pathway. Adapted from "Extrinsic and Intrinsic Apoptosis" by BioRender.com (2023). Retrieved from https//app.biorender.com/biorender-templates.

The final category, the effectors, includes members Bak, Bax and BOK, which contain domains BH1–3 [167, 168]. The initiation of the intrinsic pathway depends on Bak and/or Bax activation at the outer mitochondrial membrane. Accordingly, activated pro-apoptotic members are necessary to form Bak-Bax pores in the mitochondrial outer membrane. Furthermore, pro-apoptotic members can either activate Bak or Bax directly, which is mainly the case for Bid and Bim, or inhibit anti-apoptotic proteins upon binding, which is the case for Bad, Bik, Hrk, Noxa, and Puma [167-169]. The balance between these pro- and anti-apoptotic proteins determines

the outcome of the apoptotic process. If the process proceeds, MOMP will release potentially lethal proteins from the membrane via the Bak-Bax pores into the cytoplasm [167, 168, 170]. One example is cytochrome c which, after release, associates with APAF-1 and forms so-called apoptosomes. The apoptosome, in turn, activates caspase-9, which initiates the activation of caspase-3, caspase-6, and caspase-7, which follows the same end-route to cell death as for the extrinsic pathway (**Figure 3**) [167, 168, 170].

Post irradiation, it has been demonstrated how p53 can activate the transcription of pro-apoptotic genes belonging to the Bcl-2 family and genes encoding APAF-1 and caspase-6 that are involved in the execution of the final phases [171-174].

In malignancies which possess an altered p53, cell death due to irradiation occurs mainly via mitotic catastrophe [175, 176]. Cell death that arises during or as a consequence of abnormal mitosis is called a mitotic catastrophe, and is categorized as one of the non-apoptotic pathways of cell death [177]. Specifically, mitotic catastrophe may occur due to extensive DNA damage, problems with the mechanisms of mitosis and centrosome hyperamplification, or failure of checkpoints at the various cell cycle transitions [177-179]. In the clinic, mitotic catastrophe is considered the primary cell death mechanism in solid tumors due to radiotherapy. Compared to apoptosis, it is a delayed type of cell death, appearing days after treatment, which can explain the slow regression of solid tumors in the clinic [116, 180].

Another mechanism that can lead to cell death is the bystander effect, defined as when unirradiated cells are killed due to irradiated neighboring cells [181, 182]. Bystander cell killing has been studied in different types of cells, including tumor cells, and at various endpoints. Cells can signal to each other via direct cell-cell communication via gap junctions or extracellular cytokine signaling [182]. Extracellularly, cytokines can signal with specific ligands that activate the extrinsic pathways of apoptosis. In addition, the intrinsic pathway can also be activated via cytokine-mediated accumulation of, i.e., reactive species within the cell [182]. Several studies have observed saturation of bystander effects at doses lower than 1 Gy, as opposed to the direct effects, which increase with the dose [183, 184]. However, it has also been indicated that there may be a dose rate dependency regarding the bystander effects and its saturation [185].

Chromosomal abnormality and progression

Despite extensive DNA damage, some cells, most probably without accurate DNA damage checkpoints and altered p53, can progress and gain an increased number of aberrant chromosomes after cell division, a trait that tumor cells frequently possess [159]. These damages can occur due to radiation, where high LET radiation leads to an elevated presence of chromosomal abnormality than low LET radiation [186]. When a damaged chromosome later replicates, it can lead to, e.g., deletion, rearrangement, and amplification of chromosomal parts, subsequently increasing the mutability and genetic instability of tumor cells [187]. Subsequently, sub-clonal and heterogenic characteristics of many human cancers, specifically NB, could originate from these replicates [188]. This may also partly explain the radioresistance in relapse cases where radiotherapy has primarily been successful.

Molecular biology

From the previous sections, it has become clear that proteins are involved in various mechanisms, and more specifically, their presence and involvement are regulated by the effects of radiation. The template for a protein is found as genes in the DNA of each cell nucleus. Therefore, the cell can initiate specific protein synthesis based on certain stimuli, including radiation. Briefly, DNA is transcribed into messenger RNA (mRNA), which crosses the nuclear membrane to the cytoplasm. Once the mRNA has been transported to the ribosomes, the template can be translated, forming amino acids in a specific order, constituting protein synthesis.

The development of various methods and techniques allows one to study the biological impact of radiation at the molecular level. In this work, quantitative real-time polymerase chain reaction (qPCR) has been implemented for analyzing the expression of apoptosis-related genes, and immunohistochemical (IHC) staining has been performed to detect the presence of specific proteins.

Gene expression – qPCR

qPCR depends on fluorescence from hydrolysis probes to measure DNA amplification. Different techniques are applied to isolate RNA and

validate its purity and quality. Subsequently, RNA is converted into cDNA, and thereafter aliquoted to specific well assay plates depending on the genes of interest. The amount of a cDNA sequence in the sample is measured using fluorescent probes in the assay wells. A dedicated machine for temperature control and fluorescence readout is needed, combined with an output data analysis tool. Furthermore, since PCR only amplifies the DNA regions containing the target sequence, the method can be used to analyze samples with small amounts of DNA. Lastly, the relative changes in gene expression can be estimated by comparison with the gene expression of a reference group.

Protein markers – IHC staining

IHC staining involves localizing proteins using antibodies that bind to specific antigens. Malignancies usually overexpress certain proteins, including SSTR2, which through IHC staining, can be confirmed and lay the basis for targeted treatment. The method is widely used in the diagnosis of cancer and drug research. Briefly, the process begins with tissue fixation, which is crucial for preserving cell morphology and tissue architecture. After the sample is fixed, usually in formalin, and embedded in paraffin, sections can be sliced within 3-5 μm. The sections then go through various dehydration steps using alcohol washes. Subsequently, the sections are stained with antibodies that detect specific proteins. One of the essential difficulties is specific or non-specific staining. Hence, adding positive and negative controls for staining is a practical tool for determining specificity.

Aims

The overall aim of this work was to study the treatment potential of radiolabeled SSTAs, both as a monotherapy and in combination with an ALK-inhibitor, for children with HR-NB. All studies have been conducted preclinically, including *in vitro* (**Paper I**) and *in vivo* studies (**Papers II-IV**).

The specific aims were:

- to estimate binding and internalization of ^{177}Lu-octreotate in human neuroblastoma cell lines and compare data with other tumor types (**Paper I**)
- to develop mouse models of three xenografted HR-NB cell lines, CLB-BAR, CLB-GE and IMR-32, and determine the biodistribution and biokinetics of ^{177}Lu-octreotate in these models (**Paper II**)
- to compare the biodistribution and biokinetics between ^{177}Lu-octreotate and ^{177}Lu-octreotide in CLB-BAR bearing mice (**Paper III**)
- to study the anti-tumor effects of ^{177}Lu-octreotate and ^{177}Lu-octreotide in mice with CLB-BAR tumors (**Paper III**)
- to examine the therapeutic effects of ^{177}Lu-octreotide treatment in combination with an ALK-inhibitor, lorlatinib, in NB mouse models (**Paper IV**)
- to evaluate the expression of apoptosis-related genes after treatment with ^{177}Lu-octreotate, ^{177}Lu-octreotide, lorlatinib or ^{177}Lu-octreotide in combination with lorlatinib in mice bearing NB (**Papers III-IV**)

Materials and methods

NB cell lines (Papers I-IV)

Three aggressive human NB cell lines were included in this work: CLB-BAR, CLB-GE, and IMR-32. CLB-BAR was derived from a two-year-old girl diagnosed with a stage 4 abdominal NB and is *ALK/MYCN* amplified, with 1p deletion and 17q gain [189-191]. CLB-GE is also *ALK/MYCN* amplified [59]. IMR-32 cell line originates from an abdominal neuroblastoma mass obtained during surgery of a 13-month-old boy [192]. IMR-32 is *ALK/MYCN*-amplified with 1p deletion and 17q gain [43, 193].

Cultured tumor cells were incubated at 37°C with a medium containing a low (2 nM) or a high (10 nM) concentration of ^{177}Lu-octreotate. After 24 or 48 hours, the medium was removed from the wells and saved for activity measurements. Next, the cells were washed and incubated with trypsin and centrifuged. Subsequently, the supernatant and cell pellet (surface-bound and internalized ^{177}Lu, respectively) were separated and saved for activity measurements. Finally, cells were co-incubated with excess octreotide to study binding specificity.

Binding and internalization (Paper I)

Cultured tumor cells were incubated at 37°C with a medium containing a low (2 nM) or a high (10 nM) concentration of ^{177}Lu-octreotate. After 24 or 48 hours, the medium was removed from the wells and saved for activity measurements. Next, the cells were washed and incubated with trypsin and centrifuged. Subsequently, the supernatant and cell pellet (surface-bound and internalized ^{177}Lu, respectively) were separated and saved for activity measurements. Finally, cells were co-incubated with excess octreotide to study binding specificity (**Figure 4**).

Animal models and study design (Papers II-IV)

In our work, four to five weeks old female BALB/c nude mice (Janvier Labs, France and Charles River Laboratories, Inc, UK) were injected subcutaneously (s.c.) on their flank with 1.5-2x10^6 CLB-BAR, CLB-GE or IMR-32 cells. Approximately three to five weeks after the transplantation,

all mice had a tumor on their flank (>200 mm^3) and were included a study. In Paper II, different activity levels of ^{177}Lu-octreotate were injected intravenously (i.v.), and the biodistribution was analyzed. Mice with CLB-BAR tumor were injected with 0.15, 1.5, or 15 MBq. CLB-GE-bearing mice were injected with 0.15 or 15 MBq while IMR-32-bearing mice were administered 15 MBq (**Figure 4**). In Paper III, 1.5 or 15 MBq ^{177}Lu-octreotide was administered to CLB-BAR-bearing mice, and the biodistribution data was compared to Paper II. In the biodistribution studies (Papers II, III), mice were euthanized after 1, 24, and 168 hours and tissue samples from various organs and the tumor were collected for activity measurement (**Figure 4**).

In the therapeutic study of Paper III, 15, 30, or 60 MBq of ^{177}Lu-octreotate or ^{177}Lu-octreotide was administered to CLB-BAR-bearing mice. Paper III also included a fractionated administration where 15 MBq was divided into doses of 2x7.5 or 3x5 with two hours or one hour between each administration, respectively. In the therapeutic studies (Papers III, IV), the tumor volume for each animal was measured twice a week before and after treatment with a digital caliper. The volume of the tumor was estimated to have the shape of an ellipsoid; hence the mass was calculated based on the measured length, width, and height. In Paper III, the mice were euthanized when the tumor weight exceeded 10% of the body weight. However, in Paper IV, the mice were euthanized at specific time points (2, 7, 14 days) after the start of the treatment. In addition, tumor samples were collected for qPCR and IHC analysis (Papers III, IV). A control group was designed for every therapeutic study, in which the mice were administered saline i.v. (**Figure 4**).

Pharmaceuticals (Papers I-IV)

Both ^{177}Lu-octreotate, [^{177}Lu-DOTA^0,Tyr^3]-octreotate, (Papers I-III) and ^{177}Lu-octreotide, [^{177}Lu-DOTA^0, Tyr^3]-octreotide, (Papers III-IV) have been prepared according to the manufacturer's instructions (Mallinckrodt Medical BV, NRG, Petten, Netherlands, and Isotopen Technologien München AG, ITM, München, Germany, respectively). The specific activity of ^{177}Lu-octreotate and ^{177}Lu-octreotide was 25 and 66 MBq/µg, respectively. Radiochemical purity was measured before administration and was noted above 98% in all studies, determined by instant thin layer chromatography Silica-Gel (ITLC-SG) (chromatography paper 50/PK,

Varian, USA), with 0.1 M of sodium citrate as the mobile phase. The radiopharmaceuticals were administered i.v. to the mice.

Lorlatinib (Selleckchem, Houston, USA) was prepared with 2% DMSO, 30% PEG300, and double-distilled water (Paper IV). The solution was formulated for oral gavage as per manufacturer's instructions.

Radioactivity measurements (Papers I-IV)

To precisely determine the activity levels administered to the animal, the activity in each syringe was measured in an ionization chamber (CRC-15, Capintec, IA, USA) before and after administration.

The ^{177}Lu activity in tissue samples, $A_{tissue}(t)$, were measured by a Wallac 1480 NaI(TI) gamma counter (Wizard 3, serial no. 480036) (Papers I-II) or a PerkinElmer 2480 automatic gamma counter (Wizard 2, serial no. SGZ29160385) (Papers III-IV) using a 20% energy window centered around 208 keV. The gamma counter was calibrated against the ionization chamber and all measurement results were corrected for dead time and background radiation levels. The same equipment was also used in order to measure the ^{177}Lu activity in the supernatant and the cell pellet from the *in-vitro* studies (Paper I).

Biodistribution analyzes (Papers II & III)

The radioactivity concentration in each tissue sample, $C_{tissue}(t)$, was determined as percent of injected ^{177}Lu activity per mass of tissue (%IA/g).

$$C_{tissue}(t) = \frac{A_{tissue}(t)}{m_{tissue}\, x\, A_{\text{injected}}\,(t)}\, x\, 100\ \%,$$

Tumor-to-normal-tissue ^{177}Lu activity concentration ratios (T/N) were determined

$$\frac{T}{N}(t) = \frac{C_{tumor}\,(t)}{C_{normal\_tissue}\,(t)}.$$

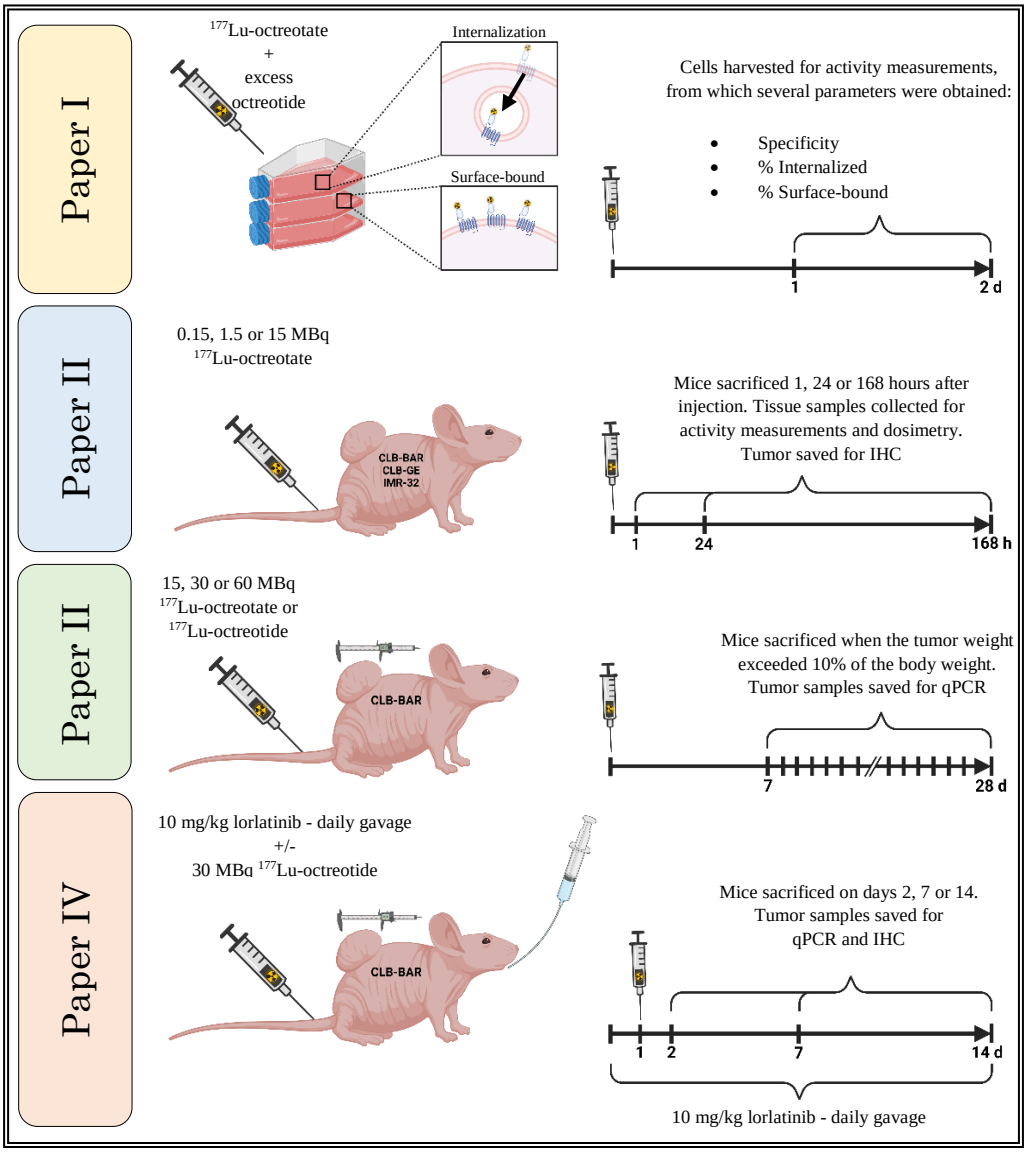

Figure 4. General study design for each project included in the thesis. Paper III also include a fractionated scheme with ^{177}Lu-octreotate described in the study design. Each treated group also had a corresponding control group (Papers III & IV).

Dosimetric analyzes (Papers II & III)

The mean absorbed dose, $\overline{D}$ for each tissue was calculated according to the equations from Medical Internal Radiation Dose (MIRD) Pamphlet No. 21 [194].

$$\overline{D} = \frac{\tilde{A}_{tissue} nE\phi}{m_{tissue}}$$

The cumulated activity for each tissue, $\tilde{A}_{tissue}$, was calculated based on the exponential function that was fitted for the activity concentrations at the various time points. For ^{177}Lu the mean energy emitted per nuclear transformation, nE, was set to 147 keV per decay. The absorbed fraction, ϕ, was set to 1.

Immunohistochemistry (Papers I-II, IV)

Tumor samples were fixed in formalin, embedded in paraffin and cut into 4 µm sections. The sections were deparaffinized, rehydrated and processed according to the manufacturer's instructions. In Papers I-II, the sections were stained with hematoxylin and eosin (H&E) and thereafter IHC stainings for SSTR1-5 and Ki67 were carried out. For positive control of SSTR1-5, tissue from human cerebellum was applied for SSTR1 and SSTR3-5, and tissue from human small intestinal NET was applied for SSTR2. In Paper IV, tumor sections were stained with cleaved caspase-3 (CC3) and evaluated by an experienced pathologist.

RNA extraction and qPCR (Papers III & IV)

RNA was isolated from each tumor sample employing a phenol-chloroform procedure. Briefly described, a small section (≤100 mg) of the frozen tumor tissue was added to a sample tube with Qiazol and thereafter lysed. Subsequently, chloroform was added, followed by various centrifugation steps, and then the aqueous phase was transferred to a new sample tube where an equal amount of 70% ethanol was added. After numerous washing steps, the RNA could be isolated. Its purity and quality, were determined for all RNA extractions, and if any of these values did not match the criteria, the extraction was repeated. The RNA was then reversely transcribed into cDNA and aliquoted into predesigned 96-well arrays for gene expression analysis. The array contains 84 key genes involved in the apoptosis pathway. The remaining 12 wells are used for controls and validation.

Based on the amount of cDNA in each well, a cycle threshold (Ct) value is recovered, where a low Ct value corresponds to high gene expression and

vice versa. The yielded Ct values from each run were then converted to ΔCt values. Subsequently, the mean relative ΔΔCt was determined for each treatment compared with the mean ΔCt of the control group. By implementing the $2^{-\Delta\Delta Ct}$ method, treated *vs.* control, we obtained a fold change (FC) value for each gene [195]. Genes were defined as differentially expressed if $|FC| > 1.5$.

Statistical analyses (Papers II-IV)

All calculations and statistical analyses were made with GraphPad Prism 9.4.1.681 (GraphPad Software, CA, USA) and Excel 2013 for Windows (Microsoft Corporation, WA, USA). The relative tumor volume (RTV) was determined individually for each mouse and time-point, and the mean value and the standard error of the mean (SEM) were calculated for each group (Papers I-IV). One-way ANOVA was used to estimate the statistical differences regarding biodistribution or tumor volume between all groups throughout the treatment period (Papers II-IV). Student t-test was applied for comparison between groups (Papers I-IV).

Results and Discussion

Different aspects must be considered when evaluating the usefulness of ^{177}Lu-labeled SSTAs for treatment of NB patients. This thesis presents data on ^{177}Lu-octreotate binding to NB cells and whether the binding is specific (Paper I). Then we also studied the internalization and retention after binding to the NB cells (Paper I). Promising in vitro results paved the way for animal studies, where different NB xenograft models were established (Paper II). Here we focused on studying the biodistribution and biokinetics of different amounts of ^{177}Lu-octreotate (Paper II). We also characterized the SSTR1-5 expression in each animal model, which was consistent with the biodistribution data. We then proceeded with therapy studies for ^{177}Lu-octreotate and ^{177}Lu-octreotide, focusing on responses regarding tumor volume and specific apoptosis-related genes (Paper III). However, no evident dose-response-relationship was observed, and relatively few genes involved in apoptosis were affected after the different treatments. In Paper IV, a combination study was conducted with ^{177}Lu-octreotide and lorlatinib, demonstrating a synergistic anti-tumor effect on the tumor volume. In addition, we noted an elevated effect on the transcriptional response for the combination treatment compared to respective monotherapies. Finally, IHC-staining demonstrated an increased incidence of apoptosis in the combination treatment group.

Binding and Internalization (Paper I)

Paper I aimed to evaluate the binding and internalization characteristics of ^{177}Lu-octreotate in two human HR-NB cell lines, CLB-BAR and IMR-32, compared with other types of cancer cell lines. The cells were incubated with low (2 nM) or high concentrations (10 nM) of ^{177}Lu-octreotate, with and without an excess of octreotide (excess factor 1000), and harvested after 24 or 48 hours.

The highest level of total binding (internalized + associated to membrane) was observed after 24 hours in IMR-32 (70%, low concentration) (**Figure 5**). Higher concentrations of ^{177}Lu-octreotate resulted in reduced total binding for both cell lines. The percentage of ^{177}Lu-octreotate internalized decreased from 24 hours to 48 hours after incubation of IMR-32 cells, while the percentage associated to membrane

increased between these time-points. The opposite trend was observed for CLB-BAR cells, indicating that the binding mechanisms that prevail differ and that the pharmacokinetics is cell line dependent. The results from Paper I demonstrated a high total binding of ^{177}Lu-octreotate to the investigated NB cell lines relative to the other cancer types studied: breast cancer, NSCLC, paraganglioma and gastrointestinal stromal tumor. Additionally, the study also demonstrated that binding was specific, since excess octreotide was able to block the available SSTRs of both NB cell lines. As previously discussed, binding agonists, such as octreotate and octreotide, to SSTRs could lead to internalization followed by receptor cycling. The extent to which this occurs depends on SSTR-expression. As Paper I also illustrates, SSTR-positive cell lines have different characteristics that must be considered to be able to optimize the treatment. SSTR expression was studied for both NB cell lines and compared with positive controls for each SSTR subtype. In line with the results regarding the total binding of ^{177}Lu-octreotate, a relatively high expression of SSTRs, mainly SSTR2, was observed for the two NB cell lines.

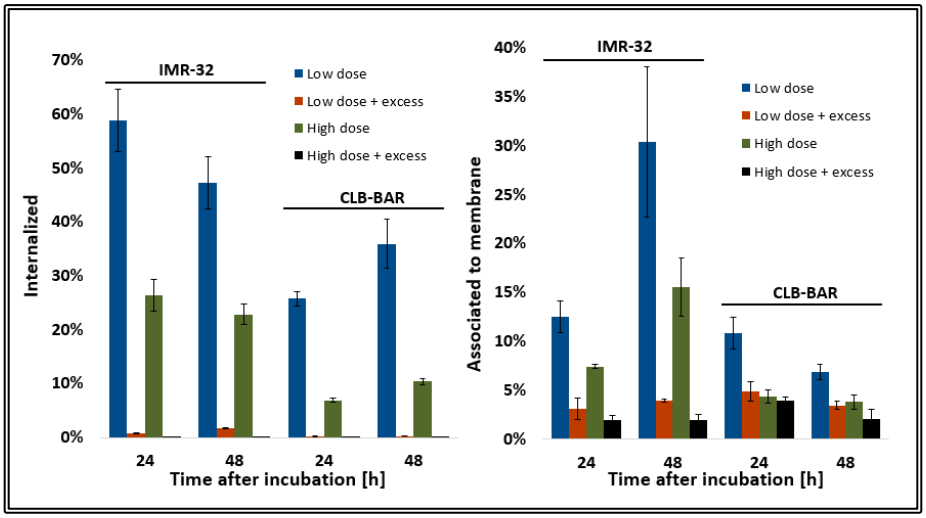

Figure 5. Percentage of ^{177}Lu-octreotate internalized and associated to the cell membrane of CLB-BAR and IMR-32 cells. The cell were incubated with low (2 nM) and high (10 nM) amounts of ^{177}Lu-octreotate, with and without an excess of free octreotide (excess factor 1000), and harvested after 24 or 48 hours.

One of the limitations regarding the study design in Paper I is that only two activity levels of ^{177}Lu-octreotate were included and that only two NB cell lines were studied. In addition, the cells were only harvested at two different time. Including more cell lines of different NB subtypes

could potentially have revealed differences in the SSTR-expression and uptake of ^{177}Lu-octreotate in different classes of NB. An increased dosage and further harvest times would have yielded a more dynamic illustration of the processes involved. Figure 3 illustrated the saturation effects of the SSTRs when a high activity level of ^{177}Lu-octreotate was administered relative to a low dose, which lead to a decrease in all studied parameters. In addition, a more suitable dosage could have been determined if additional activity levels of ^{177}Lu-octreotate were examined. However, for this study, the main questions were whether the binding is specific and whether these cell lines can be considered suitable for treatment with ^{177}Lu-labeled SSTAs, which was answered. With this in hand, only studies on tumor cells were performed in Paper I. Since we were interested in how the binding and uptake would be in a more complex model, the project proceeded with various NB xenograft models (Papers II-IV).

Biodistribution of ^{177}Lu-octreotate (Paper II)

Paper II aimed to determine the biodistribution of ^{177}Lu-octreotate in mice bearing human HR-NB. Three different cell lines were studied, CLB-BAR, CLB-GE, and IMR-32. In addition, activity dependence was studied in relation to biodistribution and mean absorbed dose.

High ^{177}Lu concentration levels were observed in all NB tumors, resulting in high tumor-to-blood (T/B) and tumor-to-kidney (T/K) ^{177}Lu concentration ratios for all three NB animal models compared with previously investigated NET animal models, e.g. GOT1 and GOT2 [196] (**Figure 6**).

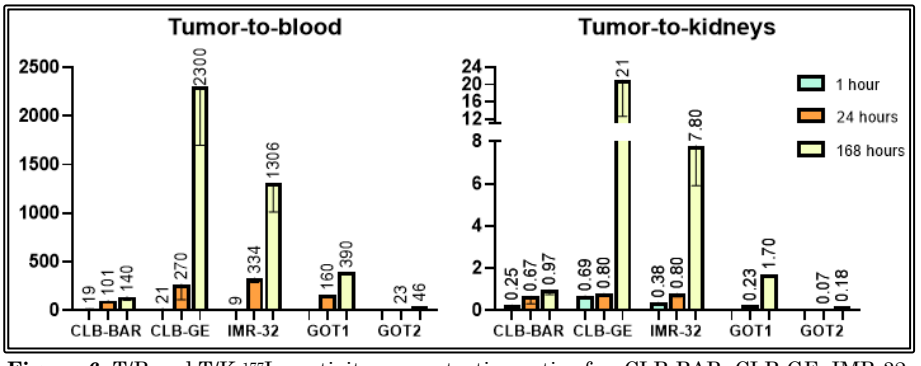

Figure 6. T/B and T/K ^{177}Lu activity concentration ratios for: CLB-BAR, CLB-GE, IMR-32, GOT1, and GOT2. The data for NB cell lines were compared with corresponding values for small intestine neuroendocrine tumor (GOT1) and medullary carcinoma (GOT2) in nude mice [196]. In all cases, 15 MBq of ^{177}Lu-octreotate was administered, except for GOT2, where 10 MBq was administered. Error bars indicate SEM.

CLB-BAR tumors had the highest uptake value of 59 %IA/g one hour post injection (p.i.) after administration of 0.15 MBq ^{177}Lu-octreotate (Paper II, Table 1).

An activity dependence could be demonstrated for CLB-BAR, where a lower administered activity (0.15 MBq) resulted in higher uptake and mean absorbed dose per injected activity (Gy/MBq) in tumor, likely due to a lower saturation of SSTRs (Paper II, Table 4). With the specific activity of 25 MBq/μg, 0.15 MBq and 15 MBq corresponds to 0.006 μg and 0.6 μg peptide, respectively. However, this was not observed for CLB-GE, where the mean absorbed dose per injected activity increased from 2.4 to 3.6 Gy/MBq with a 100-fold increase in injected activity (Paper II, Table 4). The therapeutic effect of 15 MBq can explain this trend for CLB-GE, which led to a drastic volume reduction, thus, resulting in a higher %IA/g after 168 hours (Paper II, Table 2). Although tumor volume was not measured, the mean weight of the tumors collected one week after administration can demonstrate the different responses of the tumor models. In addition, the tumors were similar in size and weight at the start of each study. The mean weights were 0.12 g, 0.29 g, and 1.9 g for the CLB-GE, IMR-32, and CLB-BAR tumors, respectively, one week after administering 15 MBq ^{177}Lu-octreotate. These results indicate that the therapeutic effect was less prominent in the CLB-BAR model. Ideally, therapy effects should be avoided in biodistribution studies aiming to compare data between different radiopharmaceuticals, since this will affect the results. However, at the same time, it is not in general correct to extrapolate biodistribution data from lower to higher activity levels, since the biodistribution of many radiopharmaceuticals depends on the peptide amount [197, 198]. This is true for tumor tissue, but in many cases also for normal tissues [199]. Since OAR are assessed as dose-limiting factors, knowledge of which injected activity that leads to highest T/N ratios is needed. However, PRRT is today usually given as fixed amount administrations or, primarily for NB patients, according to patient weight, eventually leading to undertreated patients.

The kidneys, one of the dose-limiting organs for treatment with ^{177}Lu-octreotate, were also shown in these studies to have a relatively high uptake in all xenograft models and for the different activity levels administered. Interestingly, tumor type affected the biodistribution in the organs, specifically the kidneys, demonstrated by incresed mean absorbed dose to kidneys in the studied NB xenograft models compared to other NET animal models (Paper II, Table 4). However, the other NET

models do not include an early measurement point (1-h p.i.) for estimating the mean absorbed dose to the kidneys, which may have yielded the differences [196]. Another way to extend the therapeutic window is to inhibit kidney uptake, which can be accomplished by co-administration of positively charged amino acids [200, 201]. The lungs and the adrenal glands, were the two other organs that showed relatively high uptake. These two organs also showed apparent saturation effects. For example, the lungs had a higher mean absorbed dose per injected activity than the kidneys and tumor tissue in the CLB-GE xenograft model after administration of 0.15 MBq ^{177}Lu-octreotate. Yet, a 100-fold increase in administration only led to a 5-fold increase in mean absorbed dose per injected activity. The corresponding figure for the CLB-GE tumor was a 150-fold increase in the mean absorbed dose per injected activity (Paper II, Table 4). However, as previously mentioned, there are difficulties in comparing data, since therapeutic effects on CLB-GE tumors were obtained after administration of 15 MBq ^{177}Lu-octreotate.

In order to enhance PRRT, it is necessary to have a good understanding of the cellular events induced after SSTR binding of the radiolabeled SSTA. If SSTR expression can be selectively increased in the tumor cells, the same administered activity can lead to an increased mean absorbed dose to the tumor without additional damage to normal tissue. Different ways to increase SSTR expression in tumor cells have been studied to increase the therapeutic effect. For example, up-regulation of SSTRs at the transcriptional level has been demonstrated after irradiation and pre-treatment with epigenetic modifiers [202-204].

Although all studied cell lines in Paper II were categorized as NBs, the results clearly illustrate how the tumor uptake and retention differ, highlighting the need to evaluate their tumor-specific features. One prerequisite feature for PRRT with SSTAs is the over-expression of SSTRs, which was demonstrated in Papers I and II. Similar to Paper I, the IHC staining for SSTRs was partly in line with the biodistribution data (Paper II, Figure 5).

CLB-GE tumors were found to have the most specific and intense expression of SSTR2 (**Figure 7**), which also correlated with the highest tumor uptake and hence the highest T/N values. However, contrary to the biodistribution data, our IHC-staining indicated a relatively higher SSTR2 expression for CLB-BAR xenografts than IMR-32. Similar expression patterns were seen for the other SSTR subtypes. This demonstrates that relying solely on SSTR expression to predict uptake may be an incorrect assumption. As previously mentioned, factors that play a role are the behavior of each SSTR subtype after binding the radiolabeled SSTA and the proliferation rate of the tumor cells.

All NB xenograft models were planned to receive activity levels of 0.15, 1.5, and 15 MBq. However, we had to exclude some activity levels for CLB-GE and IMR-32. Because we had difficulties with the tumor development within these two tumor models, this. Despite this, Paper II clearly demonstrates the high tumor uptake for all NB xenograft models compared to other established NET models, highlighting the potential of ^{177}Lu-octreotate as a treatment option for patients with disseminated SSTR2-positive HR-NB. In order to evaluate the therapeutic benefits of ^{177}Lu-labeled SSTAs, we planned for studies focusing on the therapeutic response in NB-bearing mice (Papers III & IV).

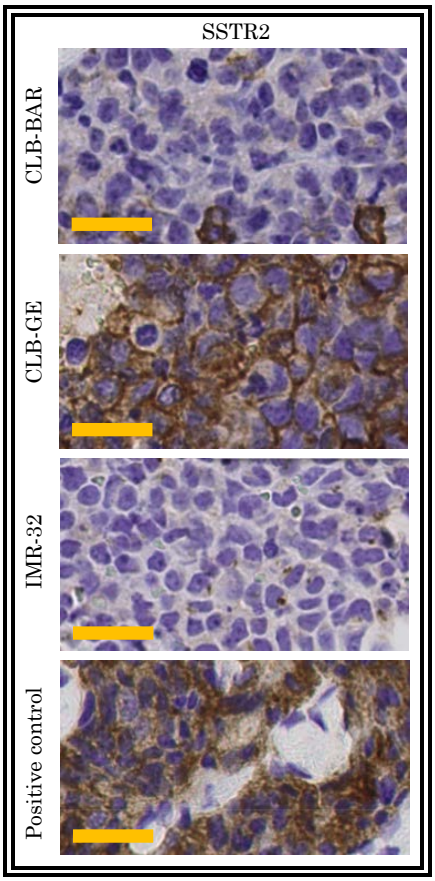

Figure 7. IHC staining for SSTR2 in CLB-BAR, CLB-GE and IMR-32. Tissues were stained with H&E prior to staining for SSTR2. For positive control, tissue from human small intestinal NET was applied. Antibody: rabbit anit-SSTR2 (1:50, ab134152, Abcam, UK). Bar equals 25 μm.

^{177}Lu-octreotate *vs.* ^{177}Lu-octreotide (Paper III)

Paper III aimed to compare the differences regarding biodistribution and the therapeutic effects of ^{177}Lu-octreotate and ^{177}Lu-octreotide in CLB-BAR xenografted mice, and to evaluate the expression of apoptosis-related genes after respective treatment.

^{177}Lu-octreotide was labeled according to the manufacturer's instructions, resulting in a specific activity of 66 MBq/µg, 2.6-fold higher than for ^{177}Lu-octreotate. Since the same activity levels were injected, different amounts of peptide were administered. The difference in peptide amount affects the biodistribution, aggravating the comparison of the studied SSTAs. However, comparing the two radiopharmaceuticals also includes their current labeling processes, which in our studies resulted in a 2.6-fold higher specific activity for ^{177}Lu-octreotide.

Analyzing the biodistribution data, a higher uptake of ^{177}Lu-octreotate was demonstrated in tumor tissue. This is in line with the affinity profiles of octreotate and octreotide towards SSTR2, which is the subtype that is most elevated in CLB-BAR tumor regarding mRNA- and receptor expression [85, 205-207]. However, the uptake was even higher in most of the other organs, hence the highest T/N ratios were observed for ^{177}Lu-octreotide (Paper III, Table 2). With focus on the blood (T/B) and the kidneys (T/K), presented in **Figure 8**. Unfortunately, bone marrow was not collected in the study with ^{177}Lu-octreotate. **Table 4** illustrates that one can underestimate the mean absorbed dose to bone marrow if one assumes that a dose estimation to the blood corresponds to bone marrow.

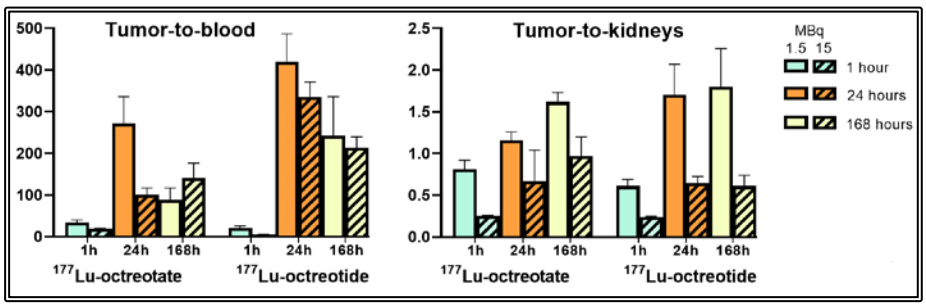

Figure 8. Tumor-to-blood and tumor-to-kidney ^{177}Lu activity concentration ratios for CLB-BAR bearing mice, 1, 24 and 168 hours post injection with ^{177}Lu-octreotate or ^{177}Lu-octreotide (1.5 or 15 MBq) [205]. Error bars represent SEM.

Although T/N ratios were greater for ^{177}Lu-octreotide in some of the comparisons, the actual concentration of ^{177}Lu, %IA/g, was, in general, higher for ^{177}Lu-octreotate in CLB-BAR tumors. Thus, ^{177}Lu-octreotate yielded an elevated mean absorbed dose to the majority of organs studied, including the OAR (**Table 4**). A 10-fold increase in injected activity of ^{177}Lu-octreotate increased the mean absorbed dose to the tumor from 4.4 to 6.8 Gy. Corresponding figures for ^{177}Lu-octreotide were 1.1 to 4.5 Gy, illustrating variable saturation effects due to a difference in peptide amount, with a more significant impact for ^{177}Lu-octreotate than for ^{177}Lu-octreotide. In contrast, after a 10-fold increase in activity for ^{177}Lu-octreotide, the kidneys received an 11-fold increase in the mean absorbed dose, compared with a 5-fold increase for ^{177}Lu-octreotate (**Table 4**). This highlights the need to consider how an increased specific activity affects uptake and retention in normal tissues.

Table 4. Mean absorbed dose per amount of injected activity (Gy/MBq) to blood, bone marrow, kidneys, and CLB-BAR tumor after injection with ^{177}Lu-octreotate [205] or ^{177}Lu-octreotide (present study).

Cell line Radiopharmaceutical	**CLB-BAR** ^{177}Lu-octreotate (Paper II)		**CLB-BAR** ^{177}Lu-octreotide (present study)	
Injected activity	**1.5 MBq**	**15 MBq**	**1.5 MBq**	**15 MBq**
Peptide amount	0.06 µg	0.6 µg	0.023 µg	0.23 µg
Blood	0.029	0.0061	0.0073	0.0058
Bone marrow	-	-	0.17	0.081
Kidneys	2.7	1.3	0.65	0.72
Tumor	2.9	0.45	0.74	0.30

The therapy studies with 15, 30, and 60 MBq of ^{177}Lu-octreotate showed no statistical differences regarding RTV between each treated group and a control group over the total treatment period (Paper III, Figure 2). However, decrease in RTV was observed for ^{177}Lu-octreotide with a statistically significant difference between the treated mice and control (Paper III, Figure 2). However, no difference was observed between the treatment groups (15, 30, and 60 MBq). Furthermore, 7-10 days post-treatment with ^{177}Lu-octreotide, the tumors started regrowth (Paper III, Figure 2). All mice were euthanized when the tumor volume exceeded 10% of the body weight, resulting in mice being euthanized on different days after the start of treatment, ranging from seven to 28 days.

The fractionation scheme with different fractions of a total 15 MBq ^{177}Lu-octreotate resulted in prolonged survival for the fractionated groups (Paper III, Figure 4). Illustrated with the 50% survival fraction of 18, 14, and 11 days for 3x5 MBq, 2x7.5 MBq, and 1x15 MBq, respectively (Paper

III, Figure 4). Although there were only 1-2 hours between each fraction, an effect could be observed, which can be considered an implement to counteract the saturation effects. By giving time and allowing the recycling of SSTRs, an increased quantity of tumor cells can be targeted again, and the anti-tumor effects can be increased. Studies have illustrated SSTR2-internalization within a couple of minutes and recycling within 40 minutes, which might make an administration interval of one hour efficient [104, 105]. However, a statistical difference could not be observed regarding RTV for the different fractionation groups compared to single treatment with 15 MBq ^{177}Lu-octreotate (Paper III, Figure 3).

The generally modest therapy response can partly be explained by the aggressive nature of the CLB-BAR tumor. CLB-BAR is classified as an HR-NB with *MYCN/ALK* amplification. Unfortunately, HR-NB displays therapy-resistant features, with the oncogene *MYCN*, in particular, acting in a central position. MYCN is essential for impairing apoptosis and stimulating tumor growth, reducing therapeutic effects [31, 208, 209]. The lack of therapy response could also be demonstrated by the few apoptosis-related genes that were regulated after the treatments (Paper III, Figure 5). Only six unique genes related to apoptosis, out of 84 genes studied, were noted to be regulated. Four of these were classified as pro-apoptotic, one as apoptosis-related, and one as anti-apoptotic (Paper III, Figure 6). Since mice in this study were euthanized at the earliest after seven days and up to 28 days after treatment, we may have missed the window where gene regulation regarding apoptosis culminated. Gene regulation is a complex and dynamic function that modifies with time. Therefore, an additional aspect of the qPCR data is that mice from the same group were euthanized at different times, presumably restricting the results.

Another limiting factor is that we only focused on 84 specific genes. Studying the entire genome and mapping all signaling pathways would have been interesting. However, it would have required significantly more time and resources as these predetermined gene arrays are much faster and advantageous for studying specific pathways. Otherwise, studying genes related to tumor growth would have been specifically interesting, as the tumors are in a regrowth phase when collected. Furthermore, we have yet to study how the transcriptional response corresponds to the protein expression. How genes are regulated does not necessarily mean this leads to a changed protein expression.

Combining Lorlatinib and ^{177}Lu-octreotide (Paper IV)

Paper IV aimed to examine the therapeutic effects of lorlatinib, an ALK-inhibitor, with ^{177}Lu-octreotide in CLB-BAR bearing mice and to evaluate the response on apoptosis-related genes and proteins.

The combination therapy with lorlatinib and ^{177}Lu-octreotide generated the most significant anti-tumor effect with a RTV of 0.39 on day 14 (**Figure 9**).

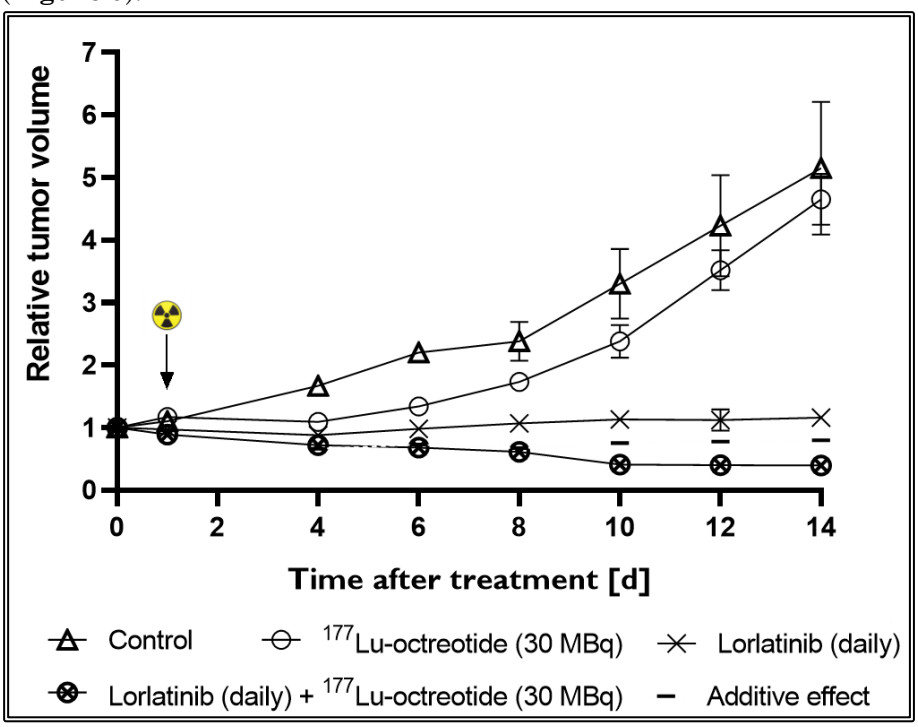

Figure 9. Effects of treatment with lorlatinib, ^{177}Lu-octreotide or their combination in mice bearing human CLB-BAR NB tumors on relative tumor volume. Mice were treated with lorlatinib (daily gavage, 10 mg/kg), and/or ^{177}Lu-octreotide (30 MBq i.v. on day 1) or i.v. injected with saline on day 1 (control) (n=10 mice/group on day 0). A theoretical additive effect was calculated using the Bliss independence model [210] and presented as a dashed line. Error bars represent SEM, not always visible due to their low values.

As monotherapies, the corresponding RTV values for lorlatinib and ^{177}Lu-octreotide were 1.2 and 4.6, respectively. The combination therapy demonstrated a more prominent anti-tumor effect than the theoretical value of the combined additive effect of both monotherapies. As indicated

by the radioactivity sign in Figure 9, ^{177}Lu-octreotide was administered on day 1, which initially had an anti-tumor effect on RTV as monotherapy, but after day 4 a steady volume increase similar to the control group was seen.

Similar to Paper III, ^{177}Lu-octreotide treatment did not have the anti-tumor effect that was expected based on the biodistribution studies and the estimated mean absorbed dose. A dose estimate based on the biodistribution data for 1.5 and 15 MBq (which resulted in 0.30 Gy/MBq for 15 MBq (**Table 4**)), estimated the corresponding ratio for 30 MBq with a continued saturation and hence decreasing value to 0.25 Gy/MBq, which results in approximately 7.5 Gy. However, this is a broad estimation of the tumor dose. With this in mind, the estimated tumor dose is relatively high, and the anti-tumor effect is less than in other NET models [211, 212], again demonstrating the radioresistant nature of this HR-NB tumor model.

The combination treatment demonstrated an elevated effect on the transcriptional response (Paper IV, Figure 4). Of the 40 regulated genes for days 2, 7, and 14, 26 belonged to the combination treatment, 10 to ^{177}Lu-octreotide, and 4 to lorlatinib (Paper IV, Figure 4). Interestingly, an elevated increase in the number of genes studied was also observed for ^{177}Lu-octreotide (30 MBq) compared to the same activity level in Paper III, ten *vs.* three. This highlights that grouping by the same time point results in additional genes detected. Another interesting trend that could be distinguished is that 16 of 18 pro-apoptotic genes were up-regulated on days 2 and 7, while all five pro-apoptotic genes were down-regulated on day 14 (Paper IV, Figure 4). As the qPCR data suggest, the substantial tumor reduction may initially correlate with an upregulation of pro-apoptotic genes. On day 14, three of these five down-regulated pro-apoptotic genes belonged to the ^{177}Lu-octreotide treatment, which aligns with the tumor growth on day 14 after treatment with ^{177}Lu-octreotide (**Figure 7**).

Before categorizing the regulated genes, according to their associated protein families, an additional statistical requirement was added to their ΔCt values (treated *vs.* control) (Paper IV, Table 1). The distinguished protein families were: TNF-superfamily, Caspase family, Bcl-2 family, TP53 family, inhibition of apoptosis (*IAP*) family, and down-regulators of CASP2,8 and p53 (Paper IV, Table 1). Two genes that were commonly found for the different treatment groups were: *CASP8*, 14 days post-

treatment-start with lorlatinib and the combination treatment, and *TNFRSF10A*, two days post-treatment-start with ^{177}Lu-octreotide and the combination treatment (Paper IV, Table 1).

A pathologist's assessment regarding the intensity and percentage of CC3-positive cells allowed the distribution of the Histoscore to be estimated (Paper IV, Figure 6). The treated groups demonstrated increased CC3-positive cells (**Figure 10**). However, this type of investigation resulted in vast spreads for each treatment, which can be reflected by the relatively distinct error bars (Paper IV, Figure 6). Ongoing studies with staining of other apoptosis markers such as Bcl-xL, Bim, and Hrk expect to provide a deeper understanding of the activated apoptosis-signaling pathways.

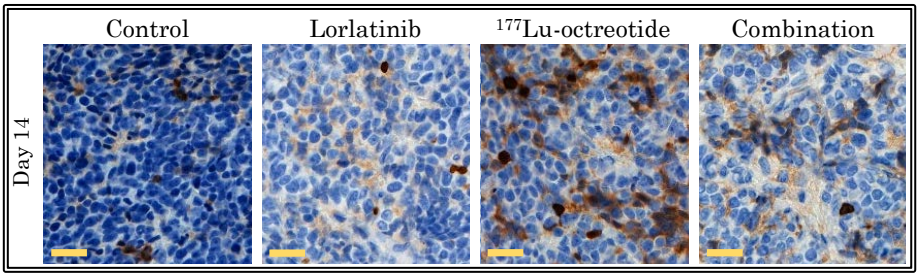

Figure 10. IHC staining for cleaved caspase-3 (CC3) in CLB-BAR tumors 14 days post respective treatment. Antibody cleaved caspase-3 (Asp175) (5A1E) Rabbit (1:100, mAb #9664, Cell Signaling Technology, Inc., USA). Bar equals 25 µm.

It would have been interesting to follow up the qPCR data with protein expression and thus be able to follow the complete path of the protein, from transcription to translation. With increased knowledge about the transcriptional response and protein expression, the investigated treatments can be further optimized by targeting the specific signaling pathways that play an essential role in the tumor response. Lorlatinib and ^{177}Lu-octreotate are in ongoing clinical phase studies for NB, separately [102, 213]. This is promising for their potential combinational use for patients with SSTR2-expressing and ALK-positive HR-NB. Although not investigated in patients, Paper IV highlights their prominent combinational effect *in vivo*.

Conclusions

This work included in this thesis contains various preclinical studies to evaluate the potential use of ^{177}Lu-labeled SSTAs, octreotate and octreotide, for treatment of NB. Furthermore, combination treatment with ^{177}Lu-labeled octreotide and an ALK-inhibitor was studied and shown to lead to a synergistic anti-tumor effect.

Summarized conclusions from each paper:

- The binding and internalization of ^{177}Lu-octreotate in the human NB cell lines, CLB-BAR and IMR-32, were specific and very high compared to other tumor cell lines of various types (**Paper I**)

- Three mouse models were developed with xenografted human HR-NB cell lines, CLB-BAR, CLB-GE, and IMR-32. The biodistribution of ^{177}Lu-octreotate in all three investigated NB models demonstrated very high tumor uptake compared to normal tissues and also compared to other established NET animal models. Consequently, ^{177}Lu-octreotate should be regarded as a potential systemic treatment option, especially in HR-NB with high expression of SSTRs (**Paper II**)

- Distinct differences in biodistribution and biokinetics were found when comparing between ^{177}Lu-octreotate and ^{177}Lu-octreotide in CLB-BAR-bearing mice. High tumor uptake of ^{177}Lu-octreotate was in general observed, resulting in a high mean absorbed dose to the tumor. However, the uptake of ^{177}Lu-octreotate was also higher in other organs. Therefore, the highest tumor-to-normal-tissue ^{177}Lu concentration ratios were observed for ^{177}Lu-octreotide (**Paper III**)

- Anti-tumor effects of ^{177}Lu-octreotate and ^{177}Lu-octreotide were studied in mice with CLB-BAR tumors. The mice receiving ^{177}Lu-octreotide displayed a more substantial anti-tumor effect than ^{177}Lu-octreotate, although the latter resulted in a higher mean absorbed dose to tumors based on the biodistribution data. The few genes that were found regulated after one to four weeks were mainly related to the extrinsic pathway for both treatments (**Paper III**)

- The therapeutic effects of ^{177}Lu-octreotide treatment in combination with an ALK-inhibitor, lorlatinib, in CLB-BAR-bearing mice demonstrated a synergistic effect. The combination therapy yielded an elevated regulation of apoptosis-related genes compared to each monotherapy. Overall, the results suggest that inhibiting ALK signaling pathways plays a role in radiosensitization of the tumor, implying a potential for clinical application of combining ALKis with radiolabeled SSTAs for HR-NBs overexpressing SSTRs and ALK (**Paper IV**)

The fact that both lorlatinib and ^{177}Lu-octreotate are in ongoing clinical phase studies for NB, separately, is promising for their potential use for patients with HR-NB. In addition, this thesis has addressed how each monotherapy and combination therapy affects apoptosis-related genes. Based on the qPCR data, treatments can be further optimized by targeting specific signaling pathways that have been shown to play an essential role in the tumor response.

Future aspects

The overall aim of this thesis was to evaluate the therapeutic potential of ^{177}Lu labeled SSTAs for treating children with HR-NB. This was done by studying different preclinical parameters, including *in vitro* and *in vivo* studies. Although the project has increased the knowledge about the uptake, biodistribution, biokinetics, and biological effects of ^{177}Lu-labeled SSTAs in NB cells and NB mouse models, numerous issues remain and should be studied further.

With the upcoming installation of new rodent-adapted SPECT and positron emission tomography (PET) systems, future biodistribution studies would become more reliable, and the same mouse would be monitored at different time points. Also, the ethical aspects regarding such animal studies would benefit, since the number of mice needed for biodistribution studies would be lower. In addition, it would be interesting to follow up and compare the data from Papers II & III with data from a rodent-adapted SPECT system.

Optimization of the peptide amount to counteract saturation effects *in vivo* is something that can enhance the treatment, both to increase anti-tumor effects but also to reduce the risk of side effects (mainly the kidneys and bone marrow). The kidneys and bone marrow samples from experiments presented in Papers III & IV are preserved in formalin and in -80° C freezer and could be used for future analyzes, especially to study potential effects of ALKi. In addition, it would be most valuable to investigate possible side effects for the studies in Papers III & IV. Using the optimized peptide amount in fractionated treatments and study the effects on the risk organs and tumors would be interesting. However, a limiting factor for performing fractionation studies is the availability of ^{177}Lu. If the treatment is to be given at daily intervals, it quickly becomes a costly arrangement. Assuming this is not a problem, an increased number of studies with different treatment schedules could help optimizing the treatment. In addition, it would be interesting to compare results from different administration schedules. Administering subsequent injections with either shorter or somewhat longer time intervals than in Paper III but still prior to the tumor regrowth phase will probably generate a more evident anti-tumor effect.

How different treatment regimens affect the transcriptional response in the tumor and normal tissues would be interesting to further investigate, since our studies only included the transcriptional response after a single injection of ^{177}Lu-labeled SSTAs. Furthermore, RNA sequencing and proteomic analyses would broaden the picture and contribute with more detailed knowledge of value for treatment optimization.

This research work was only preclinical, and data translation from mice to humans is not always straight-forward or reliable. Thus, it is important to perform clinical trials using ^{177}Lu-labled SSTAs. The few clinical studies performed or ongoing show relatively modest results. One reason is non-optimal treatment schedule. Another is radioresistance of the tumor, which might be overcome by combination treatment with e.g. lorlatinib. As previously mentioned, these drugs are already in different clinical studies, but not in combination treatment with radiopharmaceuticals. Expanding the combination studies and including other existing and clinically approved inhibitors to study their effects with radiation is very intriguing. More precisely, inhibitors of specific repair mechanisms that are involved in DDR for SSBs and DSBs should be tested. Furthermore, by locating various molecular targets and having several different treatment options, the clinic can be better prepared for patient-specific treatment options for patients with HR-NBs with drug-resistant properties. Therefore, preclinical combination studies on drug-resistant NB cell lines, particularly, are of interest and great importance.

Acknowledgments

The path to completing my Ph.D. project has not been straightforward. There have been many challenges, and I realized what previous Ph.D. students meant when they described the doctoral years as a roller coaster ride. And adding a pandemic to it does not directly downsize this description. Yet, despite this, many people around me have made work enjoyable and provided the energy to complete this journey.

First, I want to express my gratitude to my primary supervisor, Prof. Eva Forssell-Aronsson, and my co-supervisors, Prof. Bengt Hallberg and Assoc.Prof. Khalil Helou, who guided me throughout this project and offered me deep insight into the academic research.

Apart from my supervisors, I am grateful that Johan Spetz has been on board my projects. How you always made time for me during these years is something I will always take with me. You are indeed the S.I.N.H. Thanks for the time together, and good luck with the start-up of your own research group, and I hope that your Arsenal starts winning again.

I am also delighted to have shared office with Viktor Sandblom, Amin Al-Awar, and Mikael Elvborn. Warm thanks for the years together. Our conversations have been vital for me to nuance my thoughts in research and other philosophical topics. For Mikael E and Amin, I would like to say: *"Na na ni na ne!"*

I want to extend my special thanks to Rimon Thomas and Nishte Rassol. Two kind-hearted souls in our department who consistently helped me with all sorts of things. Many blessings to you both..

To all current members of the Forssell-Aronsson Lab not previously mentioned: Mikael M, Lukas L, Klara IB, Nishte R, Hana B, Anja S, and Daniella P: Thank you for creating an inspiring environment and a nice place to be in.

Appreciation to my co-authors; your contribution has raised the quality of the work, and I am very grateful for that. To colleagues at the Dept. of Medical Radiation Sciences, I wish you all the best in your work and beyond. Thank you for your time together.

I would also like to thank colleagues at Central Radionuclide Pharmacy, Experimental Biomedicine, Sahlgrenska Center for Cancer Research, especially Petra, Hamid, and Ella, respectively.

My family, you have always supported me and helped me with everyday life when needed, so that I could focus on my work when it was more demanding. Especially my sister, Armaghan, who has always been there for me, *merci tole*. And to my friends who have given me a joyful place outside work, *snett bak*.

To the love of my life, Jennifer, for your patience, support, and motivation around my work. Your belief in me has helped me when I have needed it the most. I love you!

This work was supported by grants from: The Swedish Research Council, the Swedish Cancer Society, BioCARE - a National Strategic Research Program at University of Gothenburg, the Swedish state under the agreement between the Swedish government and the county councils – the ALF-agreement, the King Gustav V Jubilee Clinic Cancer Research Foundation, the Sahlgrenska University Hospital Research Funds, Wilhelm and Martina Lundgren Research Foundation, Assar Gabrielsson Cancer Research Foundation, Herbert & Karin Jacobsson Foundation, and Adlerbertska Research Foundation.

References

1. Krenning E, Koolj P, Bakker W, Breeman W, Postema P, Kwekkeboom DJ, Oei H, de Jong M, Visser T, Reijs A: **Radiotherapy with a radiolabeled somatostatin analogue,[111In-DTPA-D-Phe1]-octreotide. A case history**. *New York Academy of Sciences Annals* 1994, **733**:496-506.
2. Pinto NR, Applebaum MA, Volchenboum SL, Matthay KK, London WB, Ambros PF, Nakagawara A, Berthold F, Schleiermacher G, Park JR *et al*: **Advances in Risk Classification and Treatment Strategies for Neuroblastoma**. *Journal of clinical oncology : official journal of the American Society of Clinical Oncology* 2015, **33**(27):3008-3017.
3. Matthay KK, Maris JM, Schleiermacher G, Nakagawara A, Mackall CL, Diller L, Weiss WA: **Neuroblastoma**. *Nat Rev Dis Primers* 2016, **2**:16078.
4. Nickerson HJ, Matthay KK, Seeger RC, Brodeur GM, Shimada H, Perez C, Atkinson JB, Selch M, Gerbing RB, Stram DO: **Favorable biology and outcome of stage IV-S neuroblastoma with supportive care or minimal therapy: a Children's Cancer Group study**. *Journal of clinical oncology* 2000, **18**(3):477-477.
5. Huang M, Weiss WA: **Neuroblastoma and MYCN**. *Cold Spring Harbor perspectives in medicine* 2013, **3**(10):a014415.
6. Brodeur GM, Bagatell R: **Mechanisms of neuroblastoma regression**. *Nature reviews Clinical oncology* 2014, **11**(12):704.
7. Maris JM: **Recent advances in neuroblastoma**. *New England Journal of Medicine* 2010, **362**(23):2202-2211.
8. Smith V, Foster J: **High-Risk Neuroblastoma Treatment Review**. *Children (Basel)* 2018, **5**(9).
9. Monclair T, Brodeur GM, Ambros PF, Brisse HJ, Cecchetto G, Holmes K, Kaneko M, London WB, Matthay KK, Nuchtern JG: **The international neuroblastoma risk group (INRG) staging system: an INRG task force report**. *Journal of clinical oncology* 2009, **27**(2):298.
10. Cohn SL, Pearson AD, London WB, Monclair T, Ambros PF, Brodeur GM, Faldum A, Hero B, Iehara T, Machin D: **The International Neuroblastoma Risk Group (INRG) classification system: an INRG task force report**. *Journal of clinical oncology* 2009, **27**(2):289.
11. Fransson S: **From 1p3 to PI3K-Studies of neuroblastoma**; 2011.
12. Kramer K, Kushner B, Heller G, Cheung NKV: **Neuroblastoma metastatic to the central nervous system: The Memorial Sloan-Kettering Cancer Center experience and a literature review**. *Cancer: Interdisciplinary International Journal of the American Cancer Society* 2001, **91**(8):1510-1519.
13. Dang CV: **MYC on the path to cancer**. *Cell* 2012, **149**(1):22-35.
14. Garson J, McIntyre P, Kemshead J: **N-myc amplification in malignant astrocytoma**. *The Lancet* 1985, **326**(8457):718-719.
15. Swartling FJ, Savov V, Persson AI, Chen J, Hackett CS, Northcott PA, Grimmer MR, Lau J, Chesler L, Perry A: **Distinct neural stem cell populations give rise to disparate brain tumors in response to N-MYC**. *Cancer cell* 2012, **21**(5):601-613.
16. Beltran H, Rickman DS, Park K, Chae SS, Sboner A, MacDonald TY, Wang Y, Sheikh KL, Terry S, Tagawa ST: **Molecular characterization of neuroendocrine prostate cancer and identification of new drug targets**. *Cancer discovery* 2011, **1**(6):487-495.
17. Liu K, Wang S, Liu Y, Gu J, Gu S, Xu Z, Zhang R, Wang Z, Ma H, Chen Y: **Overexpression of MYCN promotes proliferation of non-small cell lung cancer**. *Tumor Biology* 2016, **37**:12855-12866.
18. Brodeur GM, Seeger RC, Schwab M, Varmus HE, Bishop JM: **Amplification of N-myc in untreated human neuroblastomas correlates with advanced disease stage**. *Science* 1984, **224**(4653):1121-1124.

19. Bartolucci D, Montemurro L, Raieli S, Lampis S, Pession A, Hrelia P, Tonelli R: **MYCN impact on high-risk neuroblastoma: From diagnosis and prognosis to targeted treatment**. *Cancers* 2022, **14**(18):4421.
20. Westermark UK, Wilhelm M, Frenzel A, Henriksson MA: **The MYCN oncogene and differentiation in neuroblastoma**. In: *Seminars in cancer biology: 2011*: Elsevier; 2011: 256-266.
21. Otte J, Dyberg C, Pepich A, Johnsen JI: **MYCN function in neuroblastoma development**. *Frontiers in Oncology* 2021, **10**:624079.
22. Wenzel A, Schwab M: **The mycN/max protein complex in neuroblastoma. Short review**. *European Journal of Cancer* 1995, **31**(4):516-519.
23. Gustafson WC, Weiss WA: **Myc proteins as therapeutic targets**. *Oncogene* 2010, **29**(9):1249-1259.
24. Hansford LM, McKee AE, Zhang L, George RE, Gerstle JT, Thorner PS, Smith KM, Look AT, Yeger H, Miller FD: **Neuroblastoma cells isolated from bone marrow metastases contain a naturally enriched tumor-initiating cell**. *Cancer research* 2007, **67**(23):11234-11243.
25. Pezzolo A, Parodi F, Marimpietri D, Raffaghello L, Cocco C, Pistorio A, Mosconi M, Gambini C, Cilli M, Deaglio S: **Oct-4+/Tenascin C+ neuroblastoma cells serve as progenitors of tumor-derived endothelial cells**. *Cell research* 2011, **21**(10):1470-1486.
26. Molenaar JJ, Domingo-Fernández R, Ebus ME, Lindner S, Koster J, Drabek K, Mestdagh P, Van Sluis P, Valentijn LJ, Van Nes J: **LIN28B induces neuroblastoma and enhances MYCN levels via let-7 suppression**. *Nature genetics* 2012, **44**(11):1199-1206.
27. Flahaut M, Jauquier N, Chevalier N, Nardou K, Balmas Bourloud K, Joseph J-M, Barras D, Widmann C, Gross N, Renella R: **Aldehyde dehydrogenase activity plays a Key role in the aggressive phenotype of neuroblastoma**. *BMC cancer* 2016, **16**(1):1-13.
28. Bahmad HF, Chamaa F, Assi S, Chalhoub RM, Abou-Antoun T, Abou-Kheir W: **Cancer stem cells in neuroblastoma: expanding the therapeutic frontier**. *Frontiers in molecular neuroscience* 2019, **12**:131.
29. Tang DG: **Understanding cancer stem cell heterogeneity and plasticity**. *Cell research* 2012, **22**(3):457-472.
30. Peitzsch C, Tyutyunnykova A, Pantel K, Dubrovska A: **Cancer stem cells: The root of tumor recurrence and metastases**. In: *Seminars in cancer biology: 2017*: Elsevier; 2017: 10-24.
31. Le Grand M, Mukha A, Püschel J, Valli E, Kamili A, Vittorio O, Dubrovska A, Kavallaris M: **Interplay between MycN and c-Myc regulates radioresistance and cancer stem cell phenotype in neuroblastoma upon glutamine deprivation**. *Theranostics* 2020, **10**(14):6411.
32. Wolpaw AJ, Bayliss R, Büchel G, Dang CV, Eilers M, Gustafson WC, Hansen GH, Jura N, Knapp S, Lemmon MA: **Drugging the "undruggable" MYCN oncogenic transcription factor: overcoming previous obstacles to impact childhood cancers**. *Cancer research* 2021, **81**(7):1627-1632.
33. Rickman DS, Schulte JH, Eilers M: **The expanding world of N-MYC–driven tumors**. *Cancer discovery* 2018, **8**(2):150-163.
34. Carpenter E, Haglund E, Mace E, Deng D, Martinez D, Wood A, Chow A, Weiser D, Belcastro L, Winter C: **Antibody targeting of anaplastic lymphoma kinase induces cytotoxicity of human neuroblastoma**. *Oncogene* 2012, **31**(46):4859-4867.
35. Mossé YP, Wood A, Maris JM: **Inhibition of ALK Signaling for Cancer TherapyALK Inhibition Therapy**. *Clinical Cancer Research* 2009, **15**(18):5609-5614.
36. Hallberg B, Palmer RH: **Mechanistic insight into ALK receptor tyrosine kinase in human cancer biology**. *Nature Reviews Cancer* 2013, **13**(10):685-700.
37. Passoni L, Longo L, Collini P, Coluccia AML, Bozzi F, Podda M, Gregorio A, Gambini C, Garaventa A, Pistoia V: **Mutation-independent anaplastic lymphoma kinase overexpression in poor prognosis neuroblastoma patients**. *Cancer research* 2009, **69**(18):7338-7346.
38. Mossé YP, Laudenslager M, Longo L, Cole KA, Wood A, Attiyeh EF, Laquaglia MJ, Sennett R, Lynch JE, Perri P: **Identification of ALK as a major familial neuroblastoma predisposition gene**. *Nature* 2008, **455**(7215):930-935.

39. Bresler SC, Weiser DA, Huwe PJ, Park JH, Krytska K, Ryles H, Laudenslager M, Rappaport EF, Wood AC, McGrady PW: **ALK mutations confer differential oncogenic activation and sensitivity to ALK inhibition therapy in neuroblastoma**. *Cancer cell* 2014, **26**(5):682-694.
40. Kong X, Pan P, Sun H, Xia H, Wang X, Li Y, Hou T: **Drug discovery targeting anaplastic lymphoma kinase (ALK)**. *Journal of Medicinal Chemistry* 2019, **62**(24):10927-10954.
41. Hallberg B, Palmer R: **The role of the ALK receptor in cancer biology**. *Annals of Oncology* 2016, **27**:iii4-iii15.
42. Trigg RM, Turner SD: **ALK in neuroblastoma: biological and therapeutic implications**. *Cancers* 2018, **10**(4):113.
43. Schönherr C, Ruuth K, Kamaraj S, Wang C-L, Yang H-L, Combaret V, Djos A, Martinsson T, Christensen JG, Palmer RH: **Anaplastic Lymphoma Kinase (ALK) regulates initiation of transcription of MYCN in neuroblastoma cells**. *Oncogene* 2012, **31**(50):5193-5200.
44. Zhu S, Lee J-S, Guo F, Shin J, Perez-Atayde AR, Kutok JL, Rodig SJ, Neuberg DS, Helman D, Feng H: **Activated ALK collaborates with MYCN in neuroblastoma pathogenesis**. *Cancer cell* 2012, **21**(3):362-373.
45. Berry T, Luther W, Bhatnagar N, Jamin Y, Poon E, Sanda T, Pei D, Sharma B, Vetharoy WR, Hallsworth A: **The ALKF1174L mutation potentiates the oncogenic activity of MYCN in neuroblastoma**. *Cancer cell* 2012, **22**(1):117-130.
46. Umapathy G, Mendoza-Garcia P, Hallberg B, Palmer RH: **Targeting anaplastic lymphoma kinase in neuroblastoma**. *Apmis* 2019, **127**(5):288-302.
47. Brenner AK, Gunnes MW: **Therapeutic Targeting of the Anaplastic Lymphoma Kinase (ALK) in Neuroblastoma—A Comprehensive Update**. *Pharmaceutics* 2021, **13**(9):1427.
48. Cui JJ, Tran-Dubé M, Shen H, Nambu M, Kung P-P, Pairish M, Jia L, Meng J, Funk L, Botrous I: **Structure based drug design of crizotinib (PF-02341066), a potent and selective dual inhibitor of mesenchymal–epithelial transition factor (c-MET) kinase and anaplastic lymphoma kinase (ALK)**. *Journal of medicinal chemistry* 2011, **54**(18):6342-6363.
49. Shaw AT, Kim D-W, Nakagawa K, Seto T, Crinó L, Ahn M-J, De Pas T, Besse B, Solomon BJ, Blackhall F: **Crizotinib versus chemotherapy in advanced ALK-positive lung cancer**. *New England Journal of Medicine* 2013, **368**(25):2385-2394.
50. Choi YL, Soda M, Yamashita Y, Ueno T, Takashima J, Nakajima T, Yatabe Y, Takeuchi K, Hamada T, Haruta H: **EML4-ALK mutations in lung cancer that confer resistance to ALK inhibitors**. *New England Journal of Medicine* 2010, **363**(18):1734-1739.
51. Marsilje TH, Pei W, Chen B, Lu W, Uno T, Jin Y, Jiang T, Kim S, Li N, Warmuth M: **Synthesis, structure–activity relationships, and in vivo efficacy of the novel potent and selective anaplastic lymphoma kinase (ALK) inhibitor 5-Chloro-N 2-(2-isopropoxy-5-methyl-4-(piperidin-4-yl) phenyl)-N 4-(2-(isopropylsulfonyl) phenyl) pyrimidine-2, 4-diamine (LDK378) currently in phase 1 and phase 2 clinical trials**. *Journal of medicinal chemistry* 2013, **56**(14):5675-5690.
52. Kinoshita K, Kobayashi T, Asoh K, Furuichi N, Ito T, Kawada H, Hara S, Ohwada J, Hattori K, Miyagi T: **9-substituted 6, 6-dimethyl-11-oxo-6, 11-dihydro-5 H-benzo [b] carbazoles as Highly Selective and Potent Anaplastic Lymphoma Kinase Inhibitors**. *Journal of medicinal chemistry* 2011, **54**(18):6286-6294.
53. Huang W-S, Liu S, Zou D, Thomas M, Wang Y, Zhou T, Romero J, Kohlmann A, Li F, Qi J: **Discovery of brigatinib (AP26113), a phosphine oxide-containing, potent, orally active inhibitor of anaplastic lymphoma kinase**. *Journal of medicinal chemistry* 2016, **59**(10):4948-4964.
54. Friboulet L, Li N, Katayama R, Lee CC, Gainor JF, Crystal AS, Michellys P-Y, Awad MM, Yanagitani N, Kim S: **The ALK Inhibitor Ceritinib Overcomes Crizotinib Resistance in Non–Small Cell Lung CancerCeritinib and Crizotinib Resistance**. *Cancer discovery* 2014, **4**(6):662-673.
55. Katayama R, Friboulet L, Koike S, Lockerman EL, Khan TM, Gainor JF, Iafrate AJ, Takeuchi K, Taiji M, Okuno Y: **Two Novel ALK Mutations Mediate Acquired Resistance to the Next-Generation ALK Inhibitor AlectinibAcquired Resistance to Alectinib in ALK-Positive NSCLC**. *Clinical cancer research* 2014, **20**(22):5686-5696.

56. Johnson TW, Richardson PF, Bailey S, Brooun A, Burke BJ, Collins MR, Cui JJ, Deal JG, Deng Y-L, Dinh D: **Discovery of (10 R)-7-Amino-12-fluoro-2, 10, 16-trimethyl-15-oxo-10, 15, 16, 17-tetrahydro-2H-8, 4-(metheno) pyrazolo [4, 3-h][2, 5, 11]-benzoxadiazacyclotetradecine-3-carbonitrile (PF-06463922), a macrocyclic inhibitor of anaplastic lymphoma kinase (ALK) and c-ros oncogene 1 (ROS1) with preclinical brain exposure and broad-spectrum potency against ALK-resistant mutations**. *Journal of medicinal chemistry* 2014, **57**(11):4720-4744.
57. Zou HY, Friboulet L, Kodack DP, Engstrom LD, Li Q, West M, Tang RW, Wang H, Tsaparikos K, Wang J: **PF-06463922, an ALK/ROS1 inhibitor, overcomes resistance to first and second generation ALK inhibitors in preclinical models**. *Cancer cell* 2015, **28**(1):70-81.
58. Infarinato NR, Park JH, Krytska K, Ryles HT, Sano R, Szigety KM, Li Y, Zou HY, Lee NV, Smeal T: **The ALK/ROS1 Inhibitor PF-06463922 Overcomes Primary Resistance to Crizotinib in ALK-Driven NeuroblastomaPF-06463922 Overcomes Primary Resistance in Neuroblastoma**. *Cancer discovery* 2016, **6**(1):96-107.
59. Guan J, Tucker E, Wan H, Chand D, Danielson L, Ruuth K, El Wakil A, Witek B, Jamin Y, Umapathy G: **The ALK inhibitor PF-06463922 is effective as a single agent in neuroblastoma driven by expression of ALK and MYCN**. *Disease models & mechanisms* 2016, **9**(9):941-952.
60. Sasaki T, Koivunen J, Ogino A, Yanagita M, Nikiforow S, Zheng W, Lathan C, Marcoux JP, Du J, Okuda K: **A Novel ALK Secondary Mutation and EGFR Signaling Cause Resistance to ALK Kinase InhibitorsResistance Mechanisms in ALK Kinase Inhibitors**. *Cancer research* 2011, **71**(18):6051-6060.
61. Yamada T, Takeuchi S, Nakade J, Kita K, Nakagawa T, Nanjo S, Nakamura T, Matsumoto K, Soda M, Mano H: **Paracrine Receptor Activation by Microenvironment Triggers Bypass Survival Signals and ALK Inhibitor Resistance in EML4-ALK Lung Cancer CellsLigands Trigger ALK Inhibitor Resistance**. *Clinical cancer research* 2012, **18**(13):3592-3602.
62. Redaelli S, Ceccon M, Zappa M, Sharma GG, Mastini C, Mauri M, Nigoghossian M, Massimino L, Cordani N, Farina F: **Lorlatinib treatment elicits multiple on-and off-target mechanisms of resistance in ALK-driven cancer**. *Cancer research* 2018, **78**(24):6866-6880.
63. Arumugam S, Manning-Cork N, Gains J, Boterberg T, Gaze M: **The evidence for external beam radiotherapy in high-risk neuroblastoma of childhood: a systematic review**. *Clinical Oncology* 2019, **31**(3):182-190.
64. Gatcombe HG, Marcus Jr R, Katzenstein HM, Tighiouart M, Esiashvili N: **Excellent local control from radiation therapy for high-risk neuroblastoma**. *International Journal of Radiation Oncology* Biology* Physics* 2009, **74**(5):1549-1554.
65. Robbins JR, Krasin MJ, Panandiker ASP, Watkins A, Wu J, Santana VM, Furman WL, Davidoff AM, McGregor LM: **Radiation therapy as part of local control of metastatic neuroblastoma: the St Jude Children's Research Hospital experience**. *Journal of pediatric surgery* 2010, **45**(4):678-686.
66. Casey DL, Kushner BH, Cheung N-KV, Modak S, LaQuaglia MP, Wolden SL: **Local control with 21-Gy radiation therapy for high-risk neuroblastoma**. *International Journal of Radiation Oncology* Biology* Physics* 2016, **96**(2):393-400.
67. Carlin S, Mairs RJ, McCluskey AG, Tweddle DA, Sprigg A, Estlin C, Board J, George RE, Ellershaw C, Pearson AD: **Development of a real-time polymerase chain reaction assay for prediction of the uptake of meta-[131I] iodobenzylguanidine by neuroblastoma tumors**. *Clinical cancer research* 2003, **9**(9):3338-3344.
68. Olecki E, Grant CN: **MIBG in neuroblastoma diagnosis and treatment**. In: *Seminars in pediatric surgery: 2019*: Elsevier; 2019: 150859.
69. Wafelman AR, Hoefnagel CA, Maes RA, Beijnen JH: **Radioiodinated metaiodobenzylguanidine: a review of its biodistribution and pharmacokinetics, drug interactions, cytotoxicity and dosimetry**. *Eur J Nucl Med* 1994, **21**(6):545-559.
70. Kayano D, Kinuya S: **Iodine-131 metaiodobenzylguanidine therapy for neuroblastoma: reports so far and future perspective**. *ScientificWorldJournal* 2015, **2015**:189135.

71. Jakobsen AM, Andersson P, Saglik G, Andersson E, Kölby L, Erickson JD, Forssell-Aronsson E, Wängberg B, Ahlman H, Nilsson O: **Differential expression of vesicular monoamine transporter (VMAT) 1 and 2 in gastrointestinal endocrine tumours**. *The Journal of Pathology: A Journal of the Pathological Society of Great Britain and Ireland* 2001, **195**(4):463-472.
72. Gaze MN, Huxham IM, Mairs RJ, Barrett A: **Intracellular localization of metaiodobenzyl guanidine in human neuroblastoma cells by electron spectroscopic imaging**. *Int J Cancer* 1991, **47**(6):875-880.
73. Wieland DM, Swanson DP, Brown LE, Beierwaltes WH: **Imaging the adrenal medulla with an I-131-labeled antiadrenergic agent**. *Journal of nuclear medicine : official publication, Society of Nuclear Medicine* 1979, **20**(2):155-158.
74. Sisson JC, Frager MS, Valk TW, Gross MD, Swanson DP, Wieland DM, Tobes MC, Beierwaltes WH, Thompson NW: **Scintigraphic localization of pheochromocytoma**. *N Engl J Med* 1981, **305**(1):12-17.
75. Matthay KK, DeSantes K, Hasegawa B, Huberty J, Hattner RS, Ablin A, Reynolds CP, Seeger RC, Weinberg VK, Price D: **Phase I dose escalation of 131I-metaiodobenzylguanidine with autologous bone marrow support in refractory neuroblastoma**. *J Clin Oncol* 1998, **16**(1):229-236.
76. Matthay KK, Weiss B, Villablanca JG, Maris JM, Yanik GA, DuBois SG, Stubbs J, Groshen S, Tsao-Wei D, Hawkins R: **Dose escalation study of no-carrier-added 131I-metaiodobenzylguanidine for relapsed or refractory neuroblastoma: new approaches to neuroblastoma therapy consortium trial**. *Journal of Nuclear Medicine* 2012, **53**(7):1155-1163.
77. DuBois SG, Messina J, Maris JM, Huberty J, Glidden DV, Veatch J, Charron M, Hawkins R, Matthay KK: **Hematologic toxicity of high-dose iodine-131–metaiodobenzylguanidine therapy for advanced neuroblastoma**. *Journal of Clinical Oncology* 2004, **22**(12):2452-2460.
78. Schmidt M, Simon T, Hero B, Eschner W, Dietlein M, Sudbrock F, Bongartz R, Berthold F, Schicha H: **Is there a benefit of 131I-MIBG therapy in the treatment of children with stage 4 neuroblastoma?** *Nuklearmedizin-NuclearMedicine* 2006, **45**(04):145-151.
79. Krenning E, Kwekkeboom DJ, Bakker Wea, Breeman W, Kooij P, Oei H, van Hagen M, Postema P, de Jong M, Reubi J-C: **Somatostatin receptor scintigraphy with [111 In-DTPA-D-Phe 1]-and [123 I-Tyr 3]-octreotide: the Rotterdam experience with more than 1000 patients**. *European journal of nuclear medicine* 1993, **20**:716-731.
80. Moertel CL, Reubi JC, Scheithauer BS, Schaid DJ, Kvols LK: **Expression of somatostatin receptors in childhood neuroblastoma**. *American journal of clinical pathology* 1994, **102**(6):752-756.
81. Schilling FH, Bihl H, Jacobsson H, Ambros PF, Martinsson T, Borgström P, Schwarz K, Ambros IM, Treuner J, Kogner P: **Combined 111In-pentetreotide scintigraphy and 123I-mIBG scintigraphy in neuroblastoma provides prognostic information**. *Medical and Pediatric Oncology: The Official Journal of SIOP—International Society of Pediatric Oncology (Societé Internationale d'Oncologie Pédiatrique* 2000, **35**(6):688-691.
82. Georgantzi K, Tsolakis AV, Stridsberg M, Jakobson Å, Christofferson R, Janson ET: **Differentiated expression of somatostatin receptor subtypes in experimental models and clinical neuroblastoma**. *Pediatric blood & cancer* 2011, **56**(4):584-589.
83. Schilling FH, Ambros PF, Bihl H, Martinsson T, Ambros IM, Borgström P, Jacobsson H, Falkmer UG, Treuner J, Kogner P: **Absence of somatostatin receptor expression in vivo is correlated to di-or tetraploid 1p36-deleted neuroblastomas**. *Medical and Pediatric Oncology: The Official Journal of SIOP—International Society of Pediatric Oncology (Societé Internationale d'Oncologie Pédiatrique)* 2001, **36**(1):56-60.
84. Alexander N, Marrano P, Thorner P, Naranjo A, Van Ryn C, Martinez D, Batra V, Zhang L, Irwin MS, Baruchel S: **Prevalence and clinical correlations of somatostatin receptor-2 (SSTR2) expression in neuroblastoma**. *Journal of pediatric hematology/oncology* 2019, **41**(3):222.
85. Reubi JC, Schär J-C, Waser B, Wenger S, Heppeler A, Schmitt JS, Mäcke HR: **Affinity profiles for human somatostatin receptor subtypes SST1–SST5 of somatostatin radiotracers selected for scintigraphic and radiotherapeutic use**. *European journal of nuclear medicine* 2000, **27**(3):273-282.

86. Olias G, Viollet C, Kusserow H, Epelbaum J, Meyerhof W: **Regulation and function of somatostatin receptors**. *Journal of neurochemistry* 2004, **89**(5):1057-1091.
87. Kong G, Hofman MS, Murray WK, Wilson S, Wood P, Downie P, Super L, Hogg A, Eu P, Hicks RJ: **Initial experience with gallium-68 DOTA-octreotate PET/CT and peptide receptor radionuclide therapy for pediatric patients with refractory metastatic neuroblastoma**. *Journal of pediatric hematology/oncology* 2016, **38**(2):87-96.
88. Torun N: **68Ga-DOTA-TATE in neuroblastoma with marrow involvement**. *Clinical Nuclear Medicine* 2019, **44**(6):467-468.
89. Gains JE, Aldridge MD, Mattoli MV, Bomanji JB, Biassoni L, Shankar A, Gaze MN: **68Ga-DOTATATE and 123I-mIBG as imaging biomarkers of disease localisation in metastatic neuroblastoma: implications for molecular radiotherapy**. *Nuclear Medicine Communications* 2020, **41**(11):1169-1177.
90. Uusijärvi H, Bernhardt P, Rösch F, Maecke HR, Forssell-Aronsson E: **Electron-and positron-emitting radiolanthanides for therapy: aspects of dosimetry and production**. *Journal of Nuclear Medicine* 2006, **47**(5):807-814.
91. Jødal L: **Beta emitters and radiation protection**. *Acta Oncologica* 2009, **48**(2):308-313.
92. Firestone RB, Shirley VS: **Table of isotopes, 2 volume set**; 1998.
93. Bodei L, Cremonesi M, Grana CM, Fazio N, Iodice S, Baio SM, Bartolomei M, Lombardo D, Ferrari ME, Sansovini M: **Peptide receptor radionuclide therapy with 177 Lu-DOTATATE: the IEO phase I-II study**. *European journal of nuclear medicine and molecular imaging* 2011, **38**:2125-2135.
94. Kwekkeboom DJ, de Herder WW, Kam BL, van Eijck CH, van Essen M, Kooij PP, Feelders RA, van Aken MO, Krenning EP: **Treatment with the radiolabeled somatostatin analog [177Lu-DOTA0, Tyr3] octreotate: toxicity, efficacy, and survival**. *Journal of Clinical Oncology* 2008, **26**(13):2124-2130.
95. Emami B, Lyman J, Brown A, Cola L, Goitein M, Munzenrider J, Shank B, Solin L, Wesson M: **Tolerance of normal tissue to therapeutic irradiation**. *International Journal of Radiation Oncology* Biology* Physics* 1991, **21**(1):109-122.
96. Dawson LA, Kavanagh BD, Paulino AC, Das SK, Miften M, Li XA, Pan C, Ten Haken RK, Schultheiss TE: **Radiation-associated kidney injury**. *International Journal of Radiation Oncology* Biology* Physics* 2010, **76**(3):S108-S115.
97. Konijnenberg M, Melis M, Valkema R, Krenning E, de Jong M: **Radiation dose distribution in human kidneys by octreotides in peptide receptor radionuclide therapy**. *Journal of Nuclear Medicine* 2007, **48**(1):134-142.
98. Sundlöv A, Sjögreen-Gleisner K, Svensson J, Ljungberg M, Olsson T, Bernhardt P, Tennvall J: **Individualised 177 Lu-DOTATATE treatment of neuroendocrine tumours based on kidney dosimetry**. *European journal of nuclear medicine and molecular imaging* 2017, **44**:1480-1489.
99. Strosberg J, El-Haddad G, Wolin E, Hendifar A, Yao J, Chasen B, Mittra E, Kunz PL, Kulke MH, Jacene H: **Phase 3 trial of 177Lu-Dotatate for midgut neuroendocrine tumors**. *New England Journal of Medicine* 2017, **376**(2):125-135.
100. Gains JE, Bomanji JB, Fersht NL, Sullivan T, D'Souza D, Sullivan KP, Aldridge M, Waddington W, Gaze MN: **177Lu-DOTATATE molecular radiotherapy for childhood neuroblastoma**. *Journal of Nuclear Medicine* 2011, **52**(7):1041-1047.
101. Gains JE, Moroz V, Aldridge MD, Wan S, Wheatley K, Laidler J, Peet C, Bomanji JB, Gaze MN: **A phase IIa trial of molecular radiotherapy with 177-lutetium DOTATATE in children with primary refractory or relapsed high-risk neuroblastoma**. *European Journal of Nuclear Medicine and Molecular Imaging* 2020, **47**:2348-2357.
102. Sundquist F, Georgantzi K, Jarvis KB, Brok J, Koskenvuo M, Rascon J, van Noesel M, Grybäck P, Nilsson J, Braat A: **A Phase II Trial of a Personalized, Dose-Intense Administration Schedule of 177Lutetium-DOTATATE in Children With Primary Refractory or Relapsed High-Risk Neuroblastoma–LuDO-N**. *Frontiers in pediatrics* 2022:167.
103. Csaba Z, Dournaud P: **Cellular biology of somatostatin receptors**. *Neuropeptides* 2001, **35**(1):1-23.
104. Waser B, Tamma M-L, Cescato R, Maecke HR, Reubi JC: **Highly efficient in vivo agonist-induced internalization of sst2 receptors in somatostatin target tissues**. *Journal of nuclear medicine* 2009, **50**(6):936-941.

105. Jacobs S, Schulz S: **Intracellular trafficking of somatostatin receptors**. *Molecular and cellular endocrinology* 2008, **286**(1-2):58-62.
106. Tulipano G, Stumm R, Pfeiffer M, Kreienkamp H-J, Hollt V, Schulz S: **Differential β-arrestin trafficking and endosomal sorting of somatostatin receptor subtypes**. *Journal of Biological Chemistry* 2004, **279**(20):21374-21382.
107. Vija L, Dierickx L, Courbon F: **Receptor radionuclide targeting for neuroendocrine tumors (NET) diagnostic and therapy**. *Annales d'Endocrinologie* 2019, **80**(3):166-171.
108. del Olmo-Garcia MI, Prado-Wohlwend S, Andres A, Soriano JM, Bello P, Merino-Torres JF: **Somatostatin and Somatostatin Receptors: From Signaling to Clinical Applications in Neuroendocrine Neoplasms**. *Biomedicines* 2021, **9**(12):1810.
109. Fani M, Nicolas GP, Wild D: **Somatostatin receptor antagonists for imaging and therapy**. *Journal of nuclear medicine* 2017, **58**(Supplement 2):61S-66S.
110. Borgna F, Haller S, Rodriguez JMM, Ginj M, Grundler PV, Zeevaart JR, Köster U, Schibli R, van der Meulen NP, Müller C: **Combination of terbium-161 with somatostatin receptor antagonists—a potential paradigm shift for the treatment of neuroendocrine neoplasms**. *European journal of nuclear medicine and molecular imaging* 2022:1-14.
111. Dalm SU, Nonnekens J, Doeswijk GN, de Blois E, van Gent DC, Konijnenberg MW, de Jong M: **Comparison of the therapeutic response to treatment with a 177Lu-labeled somatostatin receptor agonist and antagonist in preclinical models**. *Journal of Nuclear Medicine* 2016, **57**(2):260-265.
112. Nicolas GP, Mansi R, McDougall L, Kaufmann J, Bouterfa H, Wild D, Fani M: **Biodistribution, pharmacokinetics, and dosimetry of 177Lu-, 90Y-, and 111In-labeled somatostatin receptor antagonist OPS201 in comparison to the agonist 177Lu-DOTATATE: the mass effect**. *Journal of Nuclear Medicine* 2017, **58**(9):1435-1441.
113. Wild D, Fani M, Fischer R, Del Pozzo L, Kaul F, Krebs S, Rivier JE, Reubi JC, Maecke HR, Weber WA: **Comparison of somatostatin receptor agonist and antagonist for peptide receptor radionuclide therapy: a pilot study**. *Journal of nuclear medicine* 2014, **55**(8):1248-1252.
114. Baum RP, Zhang J, Schuchardt C, Müller D, Mäcke H: **First-in-humans study of the SSTR antagonist 177Lu-DOTA-LM3 for peptide receptor radionuclide therapy in patients with metastatic neuroendocrine neoplasms: Dosimetry, safety, and efficacy**. *Journal of Nuclear Medicine* 2021, **62**(11):1571-1581.
115. Zhu W, Cheng Y, Jia R, Zhao H, Bai C, Xu J, Yao S, Huo L: **A prospective, randomized, double-blind study to evaluate the safety, biodistribution, and dosimetry of 68ga-nodaga-lm3 and 68ga-dota-lm3 in patients with well-differentiated neuroendocrine tumors**. *Journal of Nuclear Medicine* 2021, **62**(10):1398-1405.
116. Eriksson D, Stigbrand T: **Radiation-induced cell death mechanisms**. *Tumor Biology* 2010, **31**:363-372.
117. Zimmerman MA, Huang Q, Li F, Liu X, Li C-Y: **Cell death–stimulated cell proliferation: A tissue regeneration mechanism usurped by tumors during radiotherapy**. In: *Seminars in radiation oncology: 2013*: Elsevier; 2013: 288-295.
118. Hutchinson F: **Chemical changes induced in DNA by ionizing radiation**. *Progress in nucleic acid research and molecular biology* 1985, **32**:115-154.
119. Becker D, Sevilla MD: **The chemical consequences of radiation damage to DNA**. In: *Advances in radiation biology. Volume 17*, edn.: Elsevier; 1993: 121-180.
120. Jones G, Boswell T, Lee J, Milligan J, Ward J, Weinfeld M: **A comparison of DNA damages produced under conditions of direct and indirect action of radiation**. *International journal of radiation biology* 1994, **66**(5):441-445.
121. Kunkel TA, Erie DA: **DNA mismatch repair**. *Annu Rev Biochem* 2005, **74**:681-710.
122. Abbotts R, Wilson III DM: **Coordination of DNA single strand break repair**. *Free Radical Biology and Medicine* 2017, **107**:228-244.
123. Krokan HE, Bjørås M: **Base excision repair**. *Cold Spring Harbor perspectives in biology* 2013, **5**(4):a012583.
124. Schärer OD: **Nucleotide excision repair in eukaryotes**. *Cold Spring Harbor perspectives in biology* 2013, **5**(10):a012609.

125. Tounekti O, Kenani A, Foray Na, Orlowski S, Mir LM: **The ratio of single-to double-strand DNA breaks and their absolute values determine cell death pathway**. *British journal of cancer* 2001, **84**(9):1272-1279.
126. O'Driscoll M, Jeggo PA: **The role of double-strand break repair—insights from human genetics**. *Nature Reviews Genetics* 2006, **7**(1):45-54.
127. Shrivastav M, De Haro LP, Nickoloff JA: **Regulation of DNA double-strand break repair pathway choice**. *Cell research* 2008, **18**(1):134-147.
128. Shibata A, Conrad S, Birraux J, Geuting V, Barton O, Ismail A, Kakarougkas A, Meek K, Taucher-Scholz G, Löbrich M: **Factors determining DNA double-strand break repair pathway choice in G2 phase**. *The EMBO journal* 2011, **30**(6):1079-1092.
129. Huang R-X, Zhou P-K: **DNA damage response signaling pathways and targets for radiotherapy sensitization in cancer**. *Signal transduction and targeted therapy* 2020, **5**(1):60.
130. Zhou B-BS, Elledge SJ: **The DNA damage response: putting checkpoints in perspective**. *Nature* 2000, **408**(6811):433-439.
131. Jackson SP, Bartek J: **The DNA-damage response in human biology and disease**. *Nature* 2009, **461**(7267):1071-1078.
132. Liu Q, Turner KM, Alfred Yung W, Chen K, Zhang W: **Role of AKT signaling in DNA repair and clinical response to cancer therapy**. *Neuro-oncology* 2014, **16**(10):1313-1323.
133. Morgan MA, Lawrence TS: **Molecular pathways: overcoming radiation resistance by targeting DNA damage response pathways**. *Clinical Cancer Research* 2015, **21**(13):2898-2904.
134. O'Connor MJ: **Targeting the DNA damage response in cancer**. *Molecular cell* 2015, **60**(4):547-560.
135. Harashima H, Dissmeyer N, Schnittger A: **Cell cycle control across the eukaryotic kingdom**. *Trends in cell biology* 2013, **23**(7):345-356.
136. Pawlik TM, Keyomarsi K: **Role of cell cycle in mediating sensitivity to radiotherapy**. *International Journal of Radiation Oncology* Biology* Physics* 2004, **59**(4):928-942.
137. Maier P, Hartmann L, Wenz F, Herskind C: **Cellular pathways in response to ionizing radiation and their targetability for tumor radiosensitization**. *International journal of molecular sciences* 2016, **17**(1):102.
138. Dillon M, Good J, Harrington K: **Selective targeting of the G2/M cell cycle checkpoint to improve the therapeutic index of radiotherapy**. *Clinical oncology* 2014, **26**(5):257-265.
139. Soussi T, Béroud C: **Assessing TP53 status in human tumours to evaluate clinical outcome**. *Nature Reviews Cancer* 2001, **1**(3):233-239.
140. Mc Gee MM: **Targeting the mitotic catastrophe signaling pathway in cancer**. *Mediators of inflammation* 2015, **2015**.
141. Vogan K, Bernstein M, Leclerc J-M, Brisson L, Brossard J, Brodeur GM, Pelletier J, Gros P: **Absence of p53 gene mutations in primary neuroblastomas**. *Cancer research* 1993, **53**(21):5269-5273.
142. Tweddle DA, Malcolm AJ, Bown N, Pearson AD, Lunec J: **Evidence for the development of p53 mutations after cytotoxic therapy in a neuroblastoma cell line**. *Cancer research* 2001, **61**(1):8-13.
143. Tweddle DA, Pearson AD, Haber M, Norris MD, Xue C, Flemming C, Lunec J: **The p53 pathway and its inactivation in neuroblastoma**. *Cancer letters* 2003, **197**(1-2):93-98.
144. Jiang H: **Telomere shortening and ageing**. *Zeitschrift für Gerontologie und Geriatrie* 2007, **40**(5).
145. Deng Y, Chan SS, Chang S: **Telomere dysfunction and tumour suppression: the senescence connection**. *Nature reviews cancer* 2008, **8**(6):450-458.
146. Suzuki K, Mori I, Nakayama Y, Miyakoda M, Kodama S, Watanabe M: **Radiation-induced senescence-like growth arrest requires TP53 function but not telomere shortening**. *Radiation research* 2001, **155**(1):248-253.
147. Chang B-D, Broude EV, Dokmanovic M, Zhu H, Ruth A, Xuan Y, Kandel ES, Lausch E, Christov K, Roninson IB: **A senescence-like phenotype distinguishes tumor cells that undergo terminal proliferation arrest after exposure to anticancer agents**. *Cancer research* 1999, **59**(15):3761-3767.

148. Mirzayans R, Scott A, Cameron M, Murray D: **Induction of accelerated senescence by γ radiation in human solid tumor-derived cell lines expressing wild-type TP53**. *Radiation research* 2005, **163**(1):53-62.
149. Quick QA, Gewirtz DA: **An accelerated senescence response to radiation in wild-type p53 glioblastoma multiforme cells**. *Journal of neurosurgery* 2006, **105**(1):111-118.
150. Roninson IB: **Tumor cell senescence in cancer treatment**. *Cancer research* 2003, **63**(11):2705-2715.
151. Herbig U, Jobling WA, Chen BP, Chen DJ, Sedivy JM: **Telomere shortening triggers senescence of human cells through a pathway involving ATM, p53, and p21CIP1, but not p16INK4a**. *Molecular cell* 2004, **14**(4):501-513.
152. Fagagna FdAd, Reaper PM, Clay-Farrace L, Fiegler H, Carr P, Von Zglinicki T, Saretzki G, Carter NP, Jackson SP: **A DNA damage checkpoint response in telomere-initiated senescence**. *Nature* 2003, **426**(6963):194-198.
153. Li M, You L, Xue J, Lu Y: **Ionizing radiation-induced cellular senescence in normal, non-transformed cells and the involved DNA damage response: a mini review**. *Frontiers in pharmacology* 2018, **9**:522.
154. Suzuki M, Boothman DA: **Stress-induced premature senescence (SIPS)-influence of SIPS on radiotherapy**. *Journal of radiation research* 2008, **49**(2):105-112.
155. Tsai KK, Chuang EY-Y, Little JB, Yuan Z-M: **Cellular mechanisms for low-dose ionizing radiation–induced perturbation of the breast tissue microenvironment**. *Cancer research* 2005, **65**(15):6734-6744.
156. Chang J, Wang Y, Shao L, Laberge R-M, Demaria M, Campisi J, Janakiraman K, Sharpless NE, Ding S, Feng W: **Clearance of senescent cells by ABT263 rejuvenates aged hematopoietic stem cells in mice**. *Nature medicine* 2016, **22**(1):78-83.
157. Yosef R, Pilpel N, Tokarsky-Amiel R, Biran A, Ovadya Y, Cohen S, Vadai E, Dassa L, Shahar E, Condiotti R: **Directed elimination of senescent cells by inhibition of BCL-W and BCL-XL**. *Nature communications* 2016, **7**(1):11190.
158. Zhu Y, Tchkonia T, Fuhrmann-Stroissnigg H, Dai HM, Ling YY, Stout MB, Pirtskhalava T, Giorgadze N, Johnson KO, Giles CB: **Identification of a novel senolytic agent, navitoclax, targeting the Bcl-2 family of anti-apoptotic factors**. *Aging cell* 2016, **15**(3):428-435.
159. Hanahan D, Weinberg RA: **Hallmarks of cancer: the next generation**. *cell* 2011, **144**(5):646-674.
160. Jin Z, El-Deiry WS: **Overview of cell death signaling pathways**. *Cancer biology & therapy* 2005, **4**(2):147-171.
161. Prindull G: **Apoptosis in the embryo and tumorigenesis**. *European Journal of Cancer* 1995, **31**(1):116-123.
162. Wu GS, Burns TF, McDonald 3rd E, Jiang W, Meng R, Krantz ID, Kao G, Gan D-D, Zhou J-Y, Muschel R: **KILLER/DR5 is a DNA damage-inducible p53-regulated death receptor gene**. *Nature genetics* 1997, **17**(2):141-143.
163. Sheard MA, Uldrijan S, Vojtesek B: **Role of p53 in regulating constitutive and X-radiation-inducible CD95 expression and function in carcinoma cells**. *Cancer research* 2003, **63**(21):7176-7184.
164. Sheikh MS, Burns TF, Huang Y, Wu GS, Amundson S, Brooks KS, Fornace Jr AJ, El-Deiry WS: **p53-dependent and-independent regulation of the death receptor KILLER/DR5 gene expression in response to genotoxic stress and tumor necrosis factor α**. *Cancer research* 1998, **58**(8):1593-1598.
165. Scaffidi C, Fulda S, Srinivasan A, Friesen C, Li F, Tomaselli KJ, Debatin K-M, Krammer PH, Peter ME: **Two CD95 (APO-1/Fas) signaling pathways**. *The EMBO journal* 1998, **17**(6):1675-1687.
166. Chipuk JE, Moldoveanu T, Llambi F, Parsons MJ, Green DR: **The BCL-2 family reunion**. *Molecular cell* 2010, **37**(3):299-310.
167. Spetz JK, Florido MH, Fraser CS, Qin X, Choiniere J, Yu SJ, Singh R, Friesen M, Rubin LL, Salem J-E: **Heightened apoptotic priming of vascular cells across tissues and life span predisposes them to cancer therapy–induced toxicities**. *Science Advances* 2022, **8**(45):eabn6579.
168. Sarosiek KA, Chonghaile TN, Letai A: **Mitochondria: gatekeepers of response to chemotherapy**. *Trends in cell biology* 2013, **23**(12):612-619.

169. Sarosiek KA, Chi X, Bachman JA, Sims JJ, Montero J, Patel L, Flanagan A, Andrews DW, Sorger P, Letai A: **BID preferentially activates BAK while BIM preferentially activates BAX, affecting chemotherapy response**. *Molecular cell* 2013, **51**(6):751-765.
170. Tait SW, Green DR: **Mitochondria and cell death: outer membrane permeabilization and beyond**. *Nature reviews Molecular cell biology* 2010, **11**(9):621-632.
171. Alvarez S, Drané P, Meiller A, Bras M, Deguin-Chambon V, Bouvard V, May E: **A comprehensive study of p53 transcriptional activity in thymus and spleen of γ irradiated mouse: High sensitivity of genes involved in the two main apoptotic pathways**. *International journal of radiation biology* 2006, **82**(11):761-770.
172. Findley HW, Gu L, Yeager AM, Zhou M: **Expression and regulation of Bcl-2, Bcl-xl, and Bax correlate with p53 status and sensitivity to apoptosis in childhood acute lymphoblastic leukemia**. *Blood, The Journal of the American Society of Hematology* 1997, **89**(8):2986-2993.
173. Michalak E, Villunger A, Adams J, Strasser A: **In several cell types tumour suppressor p53 induces apoptosis largely via Puma but Noxa can contribute**. *Cell Death & Differentiation* 2008, **15**(6):1019-1029.
174. Fei P, El-Deiry WS: **P53 and radiation responses**. *Oncogene* 2003, **22**(37):5774-5783.
175. Ianzini F, Bertoldo A, Kosmacek EA, Phillips SL, Mackey MA: **Lack of p53 function promotes radiation-induced mitotic catastrophe in mouse embryonic fibroblast cells**. *Cancer cell international* 2006, **6**:1-8.
176. Vitale I, Senovilla L, Jemaà M, Michaud M, Galluzzi L, Kepp O, Nanty L, Criollo A, Rello-Varona S, Manic G: **Multipolar mitosis of tetraploid cells: inhibition by p53 and dependency on Mos**. *The EMBO journal* 2010, **29**(7):1272-1284.
177. Galluzzi L, Maiuri M, Vitale I, Zischka H, Castedo M, Zitvogel L, Kroemer G: **Cell death modalities: classification and pathophysiological implications**. *Cell death and differentiation* 2007, **14**(7):1237.
178. Eriksson D, Lőfroth P-O, Johansson L, Riklund KAhm, Stigbrand T: **Cell cycle disturbances and mitotic catastrophes in HeLa Hep2 cells following 2.5 to 10 Gy of ionizing radiation**. *Clinical Cancer Research* 2007, **13**(18):5501s-5508s.
179. Bourke E, Dodson H, Merdes A, Cuffe L, Zachos G, Walker M, Gillespie D, Morrison CG: **DNA damage induces Chk1-dependent centrosome amplification**. *EMBO reports* 2007, **8**(6):603-609.
180. Ruth AC, Roninson IB: **Effects of the multidrug transporter P-glycoprotein on cellular responses to ionizing radiation**. *Cancer research* 2000, **60**(10):2576-2578.
181. Prise KM, Schettino G, Folkard M, Held KD: **New insights on cell death from radiation exposure**. *The lancet oncology* 2005, **6**(7):520-528.
182. Prise KM, O'sullivan JM: **Radiation-induced bystander signalling in cancer therapy**. *Nature Reviews Cancer* 2009, **9**(5):351-360.
183. Nagasawa H, Little JB: **Induction of sister chromatid exchanges by extremely low doses of α-particles**. *Cancer research* 1992, **52**(22):6394-6396.
184. Belyakov O, Malcolmson A, Folkard M, Prise K, Michael B, thD: **Direct evidence for a bystander effect of ionizing radiation in primary human fibroblasts**. *British journal of cancer* 2001, **84**(5):674-679.
185. Boyd M, Ross SC, Dorrens J, Fullerton NE, Tan KW, Zalutsky MR, Mairs RJ: **Radiation-induced biologic bystander effect elicited in vitro by targeted radiopharmaceuticals labeled with α-, β-, and Auger electron–emitting radionuclides**. *Journal of nuclear medicine* 2006, **47**(6):1007-1015.
186. Franken NA, ten Cate R, Krawczyk PM, Stap J, Haveman J, Aten J, Barendsen GW: **Comparison of RBE values of high-LET α-particles for the induction of DNA-DSBs, chromosome aberrations and cell reproductive death**. *Radiation oncology* 2011, **6**(1):1-8.
187. Janssen A, Van Der Burg M, Szuhai K, Kops GJ, Medema RH: **Chromosome segregation errors as a cause of DNA damage and structural chromosome aberrations**. *Science* 2011, **333**(6051):1895-1898.
188. Umbreit NT, Zhang C-Z, Lynch LD, Blaine LJ, Cheng AM, Tourdot R, Sun L, Almubarak HF, Judge K, Mitchell TJ: **Mechanisms generating cancer genome complexity from a single cell division error**. *Science* 2020, **368**(6488):eaba0712.

189. Schleiermacher G, Bourdeaut F, Combaret V, Picrron G, Raynal V, Aurias A, Ribeiro A, Janoueix-Lerosey I, Delattre O: **Stepwise occurrence of a complex unbalanced translocation in neuroblastoma leading to insertion of a telomere sequence and late chromosome 17q gain**. *Oncogene* 2005, **24**(20):3377-3384.
190. Cazes A, Louis-Brennetot C, Mazot P, Dingli F, Lombard B, Boeva V, Daveau R, Cappo J, Combaret V, Schleiermacher G: **Characterization of rearrangements involving the ALK gene reveals a novel truncated form associated with tumor aggressiveness in neuroblastoma**. *Cancer research* 2013, **73**(1):195-204.
191. Fransson S, Hansson M, Ruuth K, Djos A, Berbegall A, Javanmardi N, Abrahamsson J, Palmer RH, Noguera R, Hallberg B: **Intragenic anaplastic lymphoma kinase (ALK) rearrangements: translocations as a novel mechanism of ALK activation in neuroblastoma tumors**. *Genes, Chromosomes and Cancer* 2015, **54**(2):99-109.
192. Tumilowicz JJ, Nichols WW, Cholon JJ, Greene AE: **Definition of a continuous human cell line derived from neuroblastoma**. *Cancer research* 1970, **30**(8):2110-2118.
193. Schleiermacher G, Janoueix-Lerosey I, Combaret V, Derré J, Couturier J, Aurias A, Delattre O: **Combined 24-color karyotyping and comparative genomic hybridization analysis indicates predominant rearrangements of early replicating chromosome regions in neuroblastoma**. *Cancer genetics and cytogenetics* 2003, **141**(1):32-42.
194. Bolch WE, Eckerman KF, Sgouros G, Thomas SR: **MIRD pamphlet no. 21: a generalized schema for radiopharmaceutical dosimetry—standardization of nomenclature**. *Journal of Nuclear Medicine* 2009, **50**(3):477-484.
195. Schmittgen TD, Livak KJ: **Analyzing real-time PCR data by the comparative CT method**. *Nature protocols* 2008, **3**(6):1101-1108.
196. Dalmo J, Rudqvist N, Spetz J, Laverman P, Nilsson O, Ahlman H, Forssell-Aronsson E: **Biodistribution of 177Lu-octreotate and 111In-minigastrin in female nude mice transplanted with human medullary thyroid carcinoma GOT2**. *Oncology reports* 2012, **27**(1):174-181.
197. Bernhardt P, Kölby L, Johanson V, Nilsson O, åkan Ahlman H, Forssell-Aronsson E: **Biodistribution of 111in-DTPA-D-Phe1-octreotide in tumor-bearing nude mice: influence of amount injected and route of administration**. *Nuclear medicine and biology* 2003, **30**(3):253-260.
198. Velikyan I, Sundin A, Eriksson B, Lundqvist H, Sörensen J, Bergström M, Långström B: **In vivo binding of [68Ga]-DOTATOC to somatostatin receptors in neuroendocrine tumours—impact of peptide mass**. *Nuclear medicine and biology* 2010, **37**(3):265-275.
199. Schüler E, Österlund A, Forssell-Aronsson E: **The amount of injected 177Lu-octreotate strongly influences biodistribution and dosimetry in C57BL/6N mice**. *Acta oncologica* 2016, **55**(1):68-76.
200. Rolleman EJ, Valkema R, de Jong M, Kooij PP, Krenning EP: **Safe and effective inhibition of renal uptake of radiolabelled octreotide by a combination of lysine and arginine**. *European journal of nuclear medicine and molecular imaging* 2003, **30**:9-15.
201. Kam B, Teunissen J, Krenning EP, de Herder WW, Khan S, Van Vliet E, Kwekkeboom DJ: **Lutetium-labelled peptides for therapy of neuroendocrine tumours**. *European journal of nuclear medicine and molecular imaging* 2012, **39**:103-112.
202. Veenstra MJ, van Koetsveld PM, Dogan F, Farrell WE, Feelders RA, Lamberts SW, de Herder WW, Vitale G, Hofland LJ: **Epidrug-induced upregulation of functional somatostatin type 2 receptors in human pancreatic neuroendocrine tumor cells**. *Oncotarget* 2018, **9**(19):14791.
203. Oddstig J, Bernhardt P, Nilsson O, Ahlman H, Forssell-Aronsson E: **Radiation-induced up-regulation of somatostatin receptor expression in small cell lung cancer in vitro**. *Nuclear medicine and biology* 2006, **33**(7):841-846.
204. Oddstig J, Bernhardt P, Nilsson O, Ahlman H, Forssell-Aronsson E: **Radiation induces up-regulation of somatostatin receptors 1, 2, and 5 in small cell lung cancer in vitro also at low absorbed doses**. *Cancer Biotherapy and Radiopharmaceuticals* 2011, **26**(6):759-765.
205. Romiani A, Spetz J, Shubbar E, Lind DE, Hallberg B, Palmer RH, Forssell-Aronsson E: **Neuroblastoma xenograft models demonstrate the therapeutic potential of 177Lu-octreotate**. *BMC cancer* 2021, **21**(1):1-14.

206. Van den Eynden J, Umapathy G, Ashouri A, Cervantes-Madrid D, Szydzik J, Ruuth K, Koster J, Larsson E, Guan J, Palmer RH: **Phosphoproteome and gene expression profiling of ALK inhibition in neuroblastoma cell lines reveals conserved oncogenic pathways**. *Science signaling* 2018, **11**(557):eaar5680.
207. Borenäs M, Umapathy G, Lai WY, Lind DE, Witek B, Guan J, Mendoza-Garcia P, Masudi T, Claeys A, Chuang TP: **ALK ligand ALKAL2 potentiates MYCN-driven neuroblastoma in the absence of ALK mutation**. *The EMBO Journal* 2021, **40**(3):e105784.
208. Kang J-H, Rychahou PG, Ishola TA, Qiao J, Evers BM, Chung DH: **MYCN silencing induces differentiation and apoptosis in human neuroblastoma cells**. *Biochemical and biophysical research communications* 2006, **351**(1):192-197.
209. Yogev O, Barker K, Sikka A, Almeida GS, Hallsworth A, Smith LM, Jamin Y, Ruddle R, Koers A, Webber HT: **p53 Loss in MYC-Driven Neuroblastoma Leads to Metabolic Adaptations Supporting RadioresistanceMetabolic Adaptation in High-Risk Neuroblastoma Lacking p53**. *Cancer research* 2016, **76**(10):3025-3035.
210. Bliss CI: **The toxicity of poisons applied jointly 1**. *Annals of applied biology* 1939, **26**(3):585-615.
211. Sandblom V, Spetz J, Shubbar E, Montelius M, Ståhl I, Swanpalmer J, Nilsson O, Forssell-Aronsson E: **Gemcitabine potentiates the anti-tumour effect of radiation on medullary thyroid cancer**. *Plos one* 2019, **14**(11):e0225260.
212. Spetz J, Langen B, Rudqvist N, Parris TZ, Helou K, Nilsson O, Forssell-Aronsson E: **Hedgehog inhibitor sonidegib potentiates 177 Lu-octreotate therapy of GOT1 human small intestine neuroendocrine tumors in nude mice**. *BMC cancer* 2017, **17**:1-11.
213. Goldsmith KC, Mosse YP, Kayser K, Chi Y-Y, Chioda M, Thurm HC, Chen J, Krishnaswami S, Peltz G, Granger M: **Phase 1 trial of lorlatinib in combination with topotecan/cyclophosphamide in children with ALK-driven refractory or relapsed neuroblastoma: A new approaches to neuroblastoma therapy consortium study**. In.: American Society of Clinical Oncology; 2022.